DEMOCRATIC AND POPULAR REPUBLIC OF ALGERIA
MINISTRY OF HIGH EDUCATION AND SCIENTIFIC RESEARCH
UNIVERSITY OF MOHAMED BOUDIAF - M'SILA

FACULTY OF SCIENCES
DEPARTMENT OF PHYSICS

N° : PH/MAT/04/2024

DOMAINE: SCIENCE OF MATTER
FIELD : PHYSICS
OPTION : MATERIAL PHYSICS

Memory Submitted for Obtaining
Diploma of Academic Master

By:

Ben Amara Ilyes

Bekhedda Belalia

TITLE

Estimating the Influence of Temperature on the Properties of Some Semiconductors Using the Debye and Boltzmann Models

Defended on 19/06/2024 in front of a jury composed of:

Karim Bouferrache	**University of Msila**	**Chairman**
Saber Saad Essaoud	**University of Msila**	**Supervisor**
Mohammed Elamin Ketfi	**University of Msila**	**Examiner**

Academic Year: 2023/2024

شكـر و عـرفـــا ن

أول من يشكر و يحمد آناء الليل و أطراف النهار هو العلي القهار الأول والآخر في الظاهر و الباطن، الذي أغرقنا بنعمه التي لا تحصى، و أغدق علينا يرزقه الذي لا يفنى، و أنار دروبنا فله جزيل الحمد و الثناء العظيم، هو الذي أنعم علينا إذ أرسل فينا عبده ورسوله محمد بن عبد الله عليه أزكى الصلوات و أطهر التسليم، أرسله بقرآنه المبين، فعلمنا ما لم يعلم، وحثنا على طلب العلم أينما وجد

لله الحمد كله والشكر كله أن وفقنا و ألهمنا الصبر على المشاق التي واجهتنا. والشكر موصول إلى كل معلم أفادنا بعلمه، من أولى المراحل الدراسية حتى هذه اللحظة

كما نرفع كلمة شكر إلى الدكتور المشرف صابر سعد السعود، على كل ما قدمه لنا من توجيهات ومعلومات قيمة ساهمت في إثراء موضوع دراستنا.

ونتقدم بجزيل الشكر إلى الأستاذ كتفي محمد الأمين على تفضله برئاسة لجنة المناقشة

والأستاذ بوفراش كريم على قبولها تقييم هذا العمل

وفي الأخير لا يسعنا إلا أن ندعو الله عز وجل أن يرزقنا السداد و الرشاد والعفاف والغنى و الهداية.

TABLE OF CONTENTS

CHAPITRE 02 : RESULTS AND DISCUSSION

LIST OF FIGURES

LIST OF TABLES

INTRODUCTION

Introduction

In the early 21st century, applied physics focuses primarily on finding new energy sources and improving storage technologies. Key efforts include seeking alternatives to hydrocarbons, such as solar panels, photovoltaic systems, and thermoelectric generators. These technologies rely heavily on the electronic properties of semiconductor materials [1].

Oxide perovskites are highly esteemed for their outstanding properties, making them ideal for various applications in semiconductors, energy storage [2], and other optical devices [3–8]. Notable types of perovskites (ABX3) include fluoro-perovskite (ABF3), chloro-perovskite (ABCl3), nitride-perovskite (ABN3), and oxide-perovskite (ABO3). In these compounds, "A" stands for an alkali metal, rare earth element, or alkaline earth element, "B" denotes a transition metal atom, and "X" signifies an anion [9,10]. Among the most important studies carried out on perovskite oxides we mention: CsVO3 [11–13], $CdZrO_3$[14] and $MgTiO_3$[15] perovskites compounds, wherein the thermodynamic and mechanical stability of $CdZrO_3$ and $MgTiO_3$ are confirmed, as well as the occurrence of transition in the electronic properties of these compounds for their band gaps from indirect to direct at 80 GPa for $CdZrO_3$[14] and 150 GPa for $MgTiO_3$ [15].

Due to the distinctive properties of perovskite oxides, we conducted a study aimed at investigating the structural, electronic, thermal, and thermoelectric properties of the compound SrSnO3 based on the following theories:

1. Density functional theory for studying structural and electronic properties[16–21].
2. Debye's quasi-harmonic model for treating the thermal properties[22,23].
3. Boltzmann's semi-classical model for thermoelectric properties [24].

References

[1] S S Essaoud, S M Al Azar, A A Mousa, and R S Masharfe *Phys. Scr.* **98** 035820 (2023).

[2] L Zhang, J Miao, J Li, and Q Li *Adv. Funct. Mater.* **30** 2003653 (2020).

[3] J Saddique, M Husain, N Rahman, R Khan, A Iqbal, M Sohail, S A Khattak, S N Khan, A A Khan, and A H Reshak *Mater. Sci. Semicond. Process.* **139** 106345 (2022).

[4] A Thatribud *Mater. Res. Express* **6** 095021 (2019).

[5] A Habib, M Husain, M Sajjad, N Rahman, R Khan, M Sohail, I H Ali, S Iqbal, M I Khan, and S A Ebraheem *Materials* **15** 2669 (2022).

[6] M Husain, N Rahman, R Khan, S Zulfiqar, S A Khattak, S N Khan, M Sohail, A Iqbal, A H Reshak, and A Khan *Int. J. Energy Res.* **46** 2446 (2022).

[7] G Hörsch and H J Paus *Opt. Commun.* **60** 69 (1986).

[8] S A Shah, M Husain, N Rahman, M Sohail, R Khan, A A Khan, A Ullah, S A Abdelmohsen, A M Abdelbacki, and A M El-Sabrout *RSC Adv.* **12** 8172 (2022).

[9] U Ayaz, S Shazia, A Abdullah, M Husain, N Rahman, and E Bonyah *AIP Adv.* **11** (2021).

[10] M Petrović, V Chellappan, and S Ramakrishna *Sol. Energy* **122** 678 (2015).

[11] S Sâad Essaoud, A Bouhemadou, S Maabed, S Bin-Omran, and R Khenata *Philos. Mag.* 1 (2022).

[12] A V Ishchenko, K V Ivanovskikh, I A Weinstein, R F Samigullina, and V V Platonov *Radiat. Meas.* **124** 48 (2019).

[13] J Luo, A Yang, Z Xie, J Huang, and X Zuo *J. Lumin.* **229** 117658 (2021).

[14] S Nazir, I Mahmood, N A Noor, A Laref, and M Sajjad *High Energy Density Phys.* **33** 100715 (2019).

[15] M Aslam, A Khan, M A Hashmi, M Sajjad, E Algrafy, G M Mustafa, A Mahmood, and S M Ramay *J. Mater. Res. Technol.* **9** 9965 (2020).

[16] A Görling *Phys. Rev. A* **59** 3359 (1999).

[17] P Hohenberg and W Kohn *Phys. Rev.* **136** B864 (1964).

[18] Á Nagy *Phys. Rep.* **298** 1 (1998).

[19] B T Sutcliffe *Fundam. Electron Density Density Matrix Density Funct. Theory At. Mol. Solid State* 3 (2003).

[20] R G Parr *Horiz. Quantum Chem.* 5 (1980).

[21] T A Wesołowski *Chall. Adv. Comput. Chem. Phys.* 153 n.d.

[22] A Otero-de-la-Roza, D Abbasi-Pérez, and V Luaña *Comput. Phys. Commun.* **182** 2232 (2011).

[23] A Otero-de-la-Roza and V Luaña *Comput. Phys. Commun.* **182** 1708 (2011).

[24] G K Madsen and D J Singh *Comput. Phys. Commun.* **175** 67 (2006).

CHAPTER 01/ THEORETICAL FRAMEWORK

1) The Schrödinger Equation

In 1926, the eminent physicist Erwin Schrödinger made a groundbreaking contribution to quantum mechanics by formulating the Schrödinger equation. This equation, a type of partial differential equation, serves as a cornerstone in the field of quantum theory. Its introduction marked a significant advancement in our understanding of the microscopic world.

The Schrödinger equation is pivotal because it provides a method for predicting the future behavior of quantum systems. By solving this equation, physicists can determine the wave function of a system. The wave function is a complex mathematical entity that encapsulates all the possible information about the system's state at a given moment. This includes information about the probabilities of finding particles in various positions and states of motion, as well as other physical properties.

The implications of Schrödinger's work extend far beyond theoretical physics. The Schrödinger equation has been instrumental in the development of numerous technologies, including semiconductors, lasers, and magnetic resonance imaging (MRI). It has also provided profound insights into the nature of chemical bonding, the behavior of subatomic particles, and the fundamental principles governing the universe [2–4]. The Schrödinger equation is mathematically expressed as follows:

$$H\Psi\left(\vec{R}_I, \vec{r}_i\right) = E\Psi\left(\vec{R}_I, \vec{r}_i\right)$$

The two vectors $\vec{R}_I$ and $\vec{r}_i$ are the coordinates of the nucleus (I) and of the electron (i).

H: Hamiltonian operator related to the sum of the kinetic energy and the potential energy of the system.

E: eigenvalue Energy of the system.

Ψ: wave function which depends on the coordinates of electrons and nuclei.

The Hamiltonian system, composed of both nuclei and electrons, included the kinetic energy contributions from electrons and nuclei. Additionally, it encompasses potential energies arising from electron-electron interactions, electron-nucleus interactions, and nucleus-nucleus

interactions. As a result, the comprehensive expression for the total Hamiltonian of the system is articulated as follows:

$$H = T_e + T_N + V_{ee} + V_{e-N} + V_{N-N}$$

$T_e = -\sum_i \frac{\hbar^2}{2m_i}\vec{\nabla}_i^2$ → Electronic kinetic energy (m_i the mass of electron i).

$T_n = -\sum_I \frac{\hbar^2}{2m_I}\vec{\nabla}_I^2$ → Nuclei kinetic energy (m_I the mass of the nucleus I).

$V_{N-N} = \sum_{I\neq J} \frac{Z_I Z_J e^2}{|R_I - R_J|}$ → The interaction part between the nuclei.

$V_{e-N} = \sum_{I,j} \frac{Z_I e^2}{|R_I - r_j|}$ → The nuclei-electrons interaction part.

$V_{e-e} = \sum_{i\neq j} \frac{e^2}{|r_i - r_j|}$ → The interaction part between the electrons.

$|R_\alpha - R_\beta|$ → The distance between the two nuclei α and β

$|r_i - R_\alpha|$ → The distance between the nucleus α and the electron i

$|r_i - r_j|$ → The distance between the two electrons i and j.

In practice, finding a solution to the Schrödinger equation is a complex task, and obtaining an exact solution becomes impractical, especially when dealing with systems involving a large number of moving electrons and interacting nuclei. To tackle this challenge, simplifications and approximations must be used to obtain an approximate solution that is as close to the real solution as possible. The following are some of the most notable approximations and simplifications to the Schrödinger equation:

2) Born-Oppenheimer Approximation

In 1927, physicists Max Born and Robert Oppenheimer introduced the Born-Oppenheimer approximation[5], a pivotal concept in molecular quantum mechanics. This approximation revolutionized the way scientists approach the complex problem of understanding the behavior of molecular systems by allowing the independent treatment of the motions of

atomic nuclei and electrons. The basis of this approximation lies in the significant disparity between the velocities of the two types of particles: atomic nuclei move much slower compared to the electrons, which zip around rapidly.

This approximation leverages the fact that, due to their greater mass, nuclei are almost stationary on the timescale of electron movement. As such, the electrons can be thought of as moving in a static potential created by the fixed nuclei. This separation simplifies the complex equations governing molecular systems, making them more tractable for both analytical and computational methods.

In practical terms, the Born-Oppenheimer approximation involves treating the nuclei as if they are fixed at certain positions while solving the Schrödinger equation for the electrons. The resulting electronic wave function depends parametrically on the positions of the nuclei. Once the electronic structure is determined, it is possible to then consider the movement of the nuclei. The kinetic energy of the nuclei can be ignored in the initial electronic structure calculation, focusing only on the electrons' kinetic and potential energies.

The approximation also implies that the potential energy associated with the interactions between the nuclei (denoted as Vnn) can be considered a constant when solving for the electronic states. This is because the nuclei's positions do not change appreciably over the timeframe of electronic movements.

According to the Born-Oppenheimer approximation we can rewrite the total wave function of the system $\Psi\left(\vec{R}_I{}^0, \vec{r}_i\right)$ in the form of a product of an electronic function $\Psi_e\left(\vec{R}_I{}^0, \vec{r}_i\right)$ and a nuclear function $\Psi_n\left(\vec{R}_I{}^0\right)$, thus, we can separate the motion of nuclei from that of electrons. Then the wave function is written:

$$\Psi\left(\vec{R}_I{}^0, \vec{r}_i\right) = \Psi_n\left(\vec{R}_I{}^0\right)\Psi_e\left(\vec{R}_I{}^0, \vec{r}_i\right)$$

$$\begin{cases} [T_e + V_{ee} + V_{en}]\Psi_e\left(\vec{R}_{\mathrm{I}}{}^0, \vec{r}_{\mathrm{i}}\right) = E_e\left(\vec{R}_{\mathrm{I}}{}^0\right)\Psi_e\left(\vec{R}_{\mathrm{I}}{}^0, \vec{r}_{\mathrm{i}}\right) \\ \left[T_n + V_{nn} + E_e\left(\vec{R}_{\mathrm{I}}{}^0\right)\right]\Psi_n\left(\vec{R}_{\mathrm{I}}{}^0\right) = E\Psi_n\left(\vec{R}_{\mathrm{I}}{}^0\right) \end{cases}$$

Despite implementing this simplification in the Schrödinger equation, solving the problem remains arduous and proves impractical with current mathematical methods, mainly due to the highly intricate electron-electron interaction. Consequently, additional approximations are employed to address the complexities involved.

3) Hartree and Hartree-Fock Approximations (HF)

The Hartree-Fock approximation was suggested to rectify and address the limitations of the Hartree approximation. In 1928[6,7] . Hartree proposed that all electrons should be considered identical particles moving independently, without interacting with each other (independent particle approximation [8]). In this approach, Hartree treats the interactions between electrons as particles carrying a charge, disregarding the spin state. The interactions are represented as Columbian repulsion interactions, neglecting both exchange and correlation terms. Additionally, the wave function is not "antisymmetric," as it fails to account for the Pauli exclusion principle [3,4].

The Hartree-Fock approximation was introduced to refine and overcome the limitations of the Hartree approximation. In 1928, Hartree proposed the independent particle approximation [8], where all electrons were treated as indistinguishable particles moving independently without mutual interactions. In this model, electron-electron interactions were treated as if they were charged particles, without considering spin states. Specifically, the interactions were described by Coulombic repulsion, omitting both exchange and correlation terms. Furthermore, the wave function in this approximation lacks antisymmetry, as it doesn't adhere to the Pauli exclusion principle [3,4]. The Hartree-Fock approximation was subsequently developed to include a more accurate description of electron behavior, particularly addressing the shortcomings related to neglecting electron-electron correlations and spin considerations.

$$H = \sum_i h_i$$

$$h_i = -\frac{\hbar^2}{2m_{\mathrm{i}}}\Delta_i - \sum_I \frac{Z_I e^2}{\left|\vec{r_i} - \vec{R}_{\mathrm{I}}{}^0\right|} + \frac{1}{2}\sum_j \frac{e^2}{\left|\vec{r_i} - \vec{r_j}\right|}$$

$$\Psi_e = \prod_i \Psi_i$$

$$E_e = \sum_i \varepsilon_i$$

In 1930, Fock [9] improved and modified Hartree model by substituting the wave functions of the electron with a Slater determinant[10]. This modification enabled Fock to incorporate the exchange effect, which Hartree had previously neglected. Consequently, the interaction between electrons now considers both the Coulomb interaction and the exchange effect. As a result, the former functions were replaced by anti-symmetric functions. Fock introduced the concept of spin in his treatment of electronic interactions, replacing the electronic system's wave function with a Slater determinant expressed by the following formula:

$$\Psi_{HF}(\vec{r}_1, \vec{r}_2, \vec{r}_3, \dots, \vec{r}_N) = \frac{1}{\sqrt{N_e!}} \begin{bmatrix} \psi_1(\vec{r}_1) & \psi_1(\vec{r}_2) & \psi_1(\vec{r}_3) & \cdots & \psi_1(\vec{r}_N) \\ \psi_2(\vec{r}_1) & \psi_2(\vec{r}_2) & \psi_2(\vec{r}_3) & \cdots & \psi_2(\vec{r}_N) \\ \psi_3(\vec{r}_1) & \psi_3(\vec{r}_2) & \psi_3(\vec{r}_3) & \dots & \psi_3(\vec{r}_N) \\ \vdots & \vdots & \vdots & \ddots & \vdots \\ \psi_N(\vec{r}_1) & \psi_N(\vec{r}_2) & \psi_N(\vec{r}_3) & \cdots & \psi_N(\vec{r}_N) \end{bmatrix}$$

where $\frac{1}{\sqrt{N_e!}}$ is a normalization factor.

4) Density Functional Theory (DFT):

The primary objective of Density Functional Theory (DFT) is to reformulate the electron's Hamiltonian using electron density instead of wave functions. Pioneering researchers such as Dirac [11], Slater [12], and Hohenburg, and Kohn [13] have made noteworthy contributions to this theory through their theoretical endeavors.

The inception of DFT can be traced back to the seminal works of Thomas and Fermi in 1927 [13,4]. In their groundbreaking research, they introduced the fundamental concept of expressing the total energy of an electronic system as a function of electron density. They envisioned the electronic system as a homogeneous and regular gas of electrons, undertaking a continuous partitioning of the Brillouin area. Notably, the electron correlations were not considered in this partitioning. Thomas and Fermi carried out this partitioning to establish regions where the

electron density remains constant in each part. The subsequent two formulas present expressions for the density and kinetic energy of a homogeneous electronic gas:

$$\rho = \frac{1}{3\pi^2} E_f^{\frac{3}{2}} \left(\frac{2m_e}{h^2}\right)^{\frac{3}{2}}$$

$$E_c = \frac{3}{5}\left(\frac{h^2}{2m_e}\right)(3\pi^2)^{\frac{2}{3}}\rho^{\frac{5}{2}}$$

4-1) Formalism of Density Functional Theory (DFT):

The Density Functional Theory (DFT) is a theoretical framework used to study systems with numerous interacting electrons. Unlike traditional methods that rely on analyzing the wave functions of individual electrons, DFT characterizes the system's total energy primarily in terms of its electronic density. This simplification makes DFT computationally efficient and allows for the investigation of complex systems such as molecules and solids with remarkable accuracy. The electronic density is mathematically represented by the formula:

$$\rho(\vec{r}) = \sum_{i=1}^{N} |\Psi_i(\vec{r})|^2$$

The Density Functional Theory (DFT) is based on two main theorems:

4-2) The Theorems of Hohenburg and Kohn:

Density Functional Theory is built upon the foundational principles laid out by the two theorems formulated by Hohenberg and Kohn in 1964.

4-2-1) First theorem:

The entire energy of an electronic system can be expressed as a functional dependent on the electron density for an external potential $V_{ext}(r)$. Therefore, by determining the electron density, it becomes feasible to know all the properties of the system. [3,18]

$$\boldsymbol{E}[(\vec{\boldsymbol{r}})] = \boldsymbol{F}[(\vec{\boldsymbol{r}})] + \int \boldsymbol{V}(\vec{\boldsymbol{r}})(\vec{\boldsymbol{r}})\boldsymbol{dr^3}$$

Where F [ρ] is universal functional.

The external potential and the universal functional F [ρ] are expressed in the form:

$$\boldsymbol{V_{ext}}(\vec{\boldsymbol{r_i}}) = -\sum_{\boldsymbol{A}} \frac{\boldsymbol{Z_A}}{\boldsymbol{r_{iA}}}$$

$$\boldsymbol{F}[\boldsymbol{\rho}] = \boldsymbol{T}[\boldsymbol{\rho}] + \boldsymbol{U}[\boldsymbol{\rho}]$$

Where Z_A is the charge of the nucleus, r_{iA} is the distance between nucleus A and electron i.

4-2-2) Second theorem:

The second theory states that obtining the total energy of the ground state of the electronic system, it is enough to find the corresponding electron density which makes the density function at its minimum value.

$$E\left(\rho_0(\vec{r})\right) \leq E[\rho(\vec{r})]$$

$$E(\rho_0) = MinE(\rho) \lim_{\rho \to N} \left\langle \Psi \middle| \hat{T} + \sum_i V_{ext} + V_{ee} \middle| \Psi \right\rangle$$

Obtaining the electron density corresponding to the ground state involves applying the variational principle through the differential of total energy with terms to the electron density:

$$\frac{dF[\rho(r)]}{d\rho(r)} + V(r) = 0$$

Thus, once we identify the electron density that minimizes the energy function, it becomes straightforward to ascertain the wave function and accurately determine the ground state energy.

4-3) The Kohn - Sham equation:

One of the challenges in studying systems with numerous electrons is the inability to express kinetic energy and electron-electron interactions analytically in terms of electron density. In

1965, Kohn and Sham proposed a novel approach to address this challenge. They suggested replacing the real electronic system with a hypothetical system where each electron behaves autonomously, detached from the influence of other electrons. Instead, each electron's behavior is governed by an effective potential called the Kohn-Sham potential. This potential accounts for both the external potential created by atomic nuclei and the potential resulting from the interactions of the remaining particles with the electron [3,19,20].

The Kohn-Sham fictive system is distinguished by:

The Kohn-Sham orbits which are space wave functions of a single electron are solutions of the Schrödinger equation in this vacuum space.

The fictive electronic system has the same electronic density as a real system.

The kinetic energy of the fictive system is the kinetic energy of the electrons without the correlation effect and it is positive, while the kinetic energy in the real system "T_R" is the sum of the kinetic energy of the fictive system "T_f" and an additional term that expresses the effect of the correlation "T_c" on the kinetic energy of the electron [3]:

$$T_R = T_f + T_c$$

$$T_c = \langle \Psi | T | \Psi \rangle - \langle \varphi | T_s | \varphi \rangle$$

The V_{ee} interaction between electrons in the real system which is written in the following relation:

$$\langle \Psi | V_{ee} | \Psi \rangle = U_H + U_x + U_c$$

where the terms represent:

U_H: The electronic Coulomb (Hartree potential)

U_x: The exchange energy between electrons of the same spin.

Uc: The correlation energy between the electrons.

The Kohn-Sham equation for an electronic system is given as a function of the kinetic energy of the electron: external potential energy, Hartree interaction and exchange-correlation energy as follows:

- ✓ The kinetic energy of an electron in a fictitious system:

$$T_s[\rho] = \left\langle \varphi_i \left| -\frac{\hbar^2}{2\mathrm{m}}\Delta \right| \varphi_i \right\rangle = -\frac{\hbar^2}{2\mathrm{m}} \sum_{\mathrm{i}} \int \varphi_i \nabla^2 \varphi_i^* dr_i$$

- ✓ The external potential generated by the effect of nuclei (nucleus-electron interaction):

$$V_{NE}[\rho] = -\int \sum_{I,i} \frac{Z_I \rho(\vec{r})}{\left|\vec{R}_{\mathrm{I}}^{\,0} - \vec{r}_{\mathrm{i}}\right|} dr$$

- ✓ The Hartree potential (Coulomb electron-electron interaction)

$$U[\rho] = \frac{1}{2} \int \frac{\rho(\vec{r})\rho\left(\overrightarrow{r'}\right)}{\left|\vec{r} - \overrightarrow{r'}\right|} dr dr'$$

The exchange-correlation energy, comprising both the correlation and exchange terms, lacks an exact mathematical expression. Instead, it is approximated through various methods to estimate its value.

$$E_{xc}[\rho] = E_x[\rho] + E_c[\rho]$$

And finally, the Kohn-Sham equation is written as follows [1–3]:

$$H_{KS}\varphi_i(\vec{r}) = [T_s[\rho] + V_{KS}(\vec{r})]\varphi_i(\vec{r}) = \varepsilon^{KS}\varphi_i(\vec{r})$$

$$V_{KS}(\vec{r}) = V_{ext}(\vec{r}) + V_H(\vec{r}) + +V_{XC}(\vec{r})$$

$$E[\rho] = T_s[\rho] + V_{NE}[\rho] + U_H[\rho] + E_{xc}[\rho]$$

4-3) Solution of the Kohn - Sham Equation:

Solving the Kohn-Sham equation depends on two basic steps:

Firstly, specifying all components of the effective Kohn-Sham potential, including the exchange-correlation potential (Exc), which lacks a mathematical formula but can be approximated through estimation methods.

Secondly, determining the wave functions (Kohn-Sham orbitals), which serve as solutions to the Kohn-Sham equation, expressed as: [3]:

$$\varphi_{KS}(\vec{r}) = \sum_j C_{ij}\, \varphi_j(\vec{r})$$

Where $\varphi_i(\vec{r})$ are the basic functions, and Cij are are the development coefficients.

$$\sum_j C_{ij}\, H_{KS}|\varphi_j\rangle = \sum_j C_{ij}\varepsilon_{KS}\,|\varphi_j\rangle$$

$$\langle\varphi_k|\sum_j C_{ij}\, H_{KS}|\varphi_j\rangle = \langle\varphi_k|\sum_j C_{ij}\varepsilon_{KS}\,|\varphi_j\rangle$$

$$\sum_j \quad (\langle\varphi_k|H_{KS}|\varphi_j\rangle - \varepsilon_{KS}\langle\varphi_k|\varphi_j\rangle)C_{ij} = 0$$

It remains to determine the C_{ij} coefficients.

The Kohn-Sham equation is solved according to an iterative cycles illustrated by

figure (1.I), where the process starts using an initial density ρ_infor the first iteration, this density is used to solve the Kohn-Sham equation,Subsequently, a superposition of the atomic densities is utilized to compute the Kohn-Sham matrix, facilitating the solution of the equations to obtain the Kohn-Sham orbitals.

After this step, the new density, ρ_{out}, is calculated to assess the convergence condition, checking for significant changes in density or energy. The two charge densities, ρ_{out} and ρ_{in}, are then combined through a mixing procedure, as follows:

$$\rho_{in}^{i+1} = (1 - \alpha)\rho_{in}^{i} + \rho_{out}^{i}$$

Thus the iterative procedure can be repeated until the convergence condition is fulfilled.

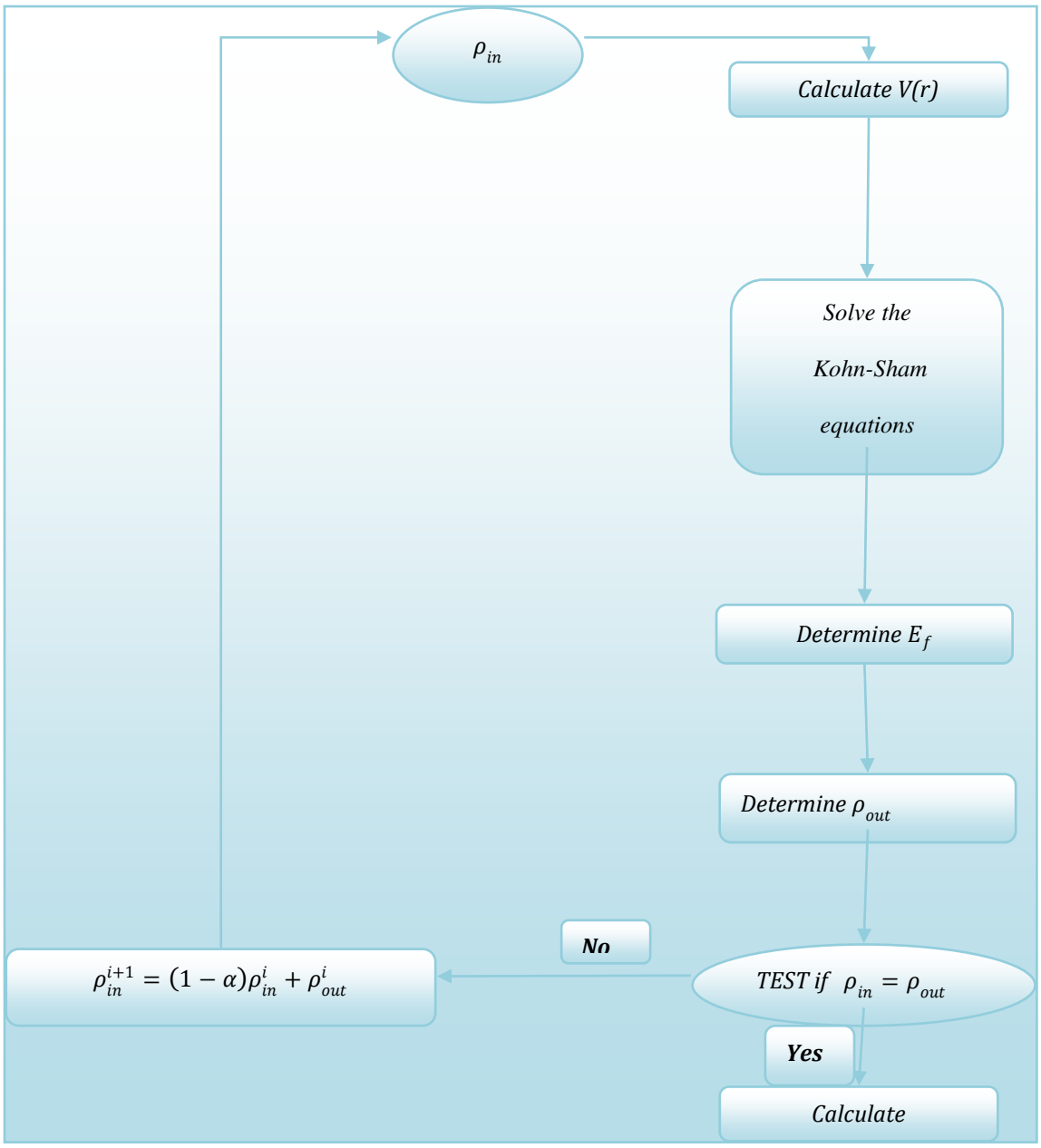

Figure I. 1: Self-consistent calculation steps.

5)The Different Types of Approximation of the $E_{xc}[\rho]$

Various methods have been utilized to estimate the values of the exchange-correlation potential between electrons due to the lack of an analytical expression. The accuracy of the results obtained relies heavily on the mathematical formulation governing this potential.

5-1) Local density approximation (LSDA)

Kohn and Sham introduced this model in 1964 [24], which entails approximating the non-uniform electronic system with a locally homogeneous electronic system by partitioning the Brillouin zone into small regions. The expression for energy exchange-correlation is subsequently determined as follows:

$$E_{XC}^{LSDA} = \int \rho(\vec{r})\, E_{xc}[\rho(\vec{r})]d\vec{r}$$

$$V_{xc} = \frac{dE_{XC}^{LDA}[\rho]}{d\rho} = \varepsilon_{XC}^{LDA} + \rho(\vec{r})\frac{d\varepsilon_{XC}^{LDA}}{d\rho}$$

For each spin up or down magnetic order, the total electron density becomes the sum of the two electron densities

$$\rho(\vec{r}) = \rho_{\uparrow}(\vec{r}) + \rho_{\downarrow}(\vec{r})$$

The Kohn-Sham equation for the two spins in the form [4]:

$$\begin{cases} \left(\frac{-\hbar^2}{2m}\nabla^2 + V_{eff}^{\uparrow}(\vec{r})\right)\varphi_i(\vec{r}) = \varepsilon_{KS}^{\uparrow}\varphi_i(\vec{r}) \\ \left(\frac{-\hbar^2}{2m}\nabla^2 + V_{eff}^{\downarrow}(\vec{r})\right)\varphi_i(\vec{r}) = \varepsilon_{KS}^{\downarrow}\varphi_i(\vec{r}) \end{cases}$$

The effective potential for the two spins is written as [4]:

$$\begin{cases} V_{eff}^{\uparrow}(\vec{r}) = V_{ext} + V_{xc}^{\uparrow} = V_{ext} + \frac{d\varepsilon_{XC}^{LSDA}[\rho_{\uparrow}(\vec{r}),\rho_{\downarrow}(\vec{r})]}{d\rho_{\uparrow}(\vec{r})} \\ V_{eff}^{\downarrow}(\vec{r}) = V_{ext} + V_{xc}^{\downarrow} = V_{ext} + \frac{d\varepsilon_{XC}^{LSDA}[\rho_{\uparrow}(\vec{r}),\rho_{\downarrow}(\vec{r})]}{d\rho_{\downarrow}(\vec{r})} \end{cases}$$

5-2) The Generalized Gradient Approximation GGA

In the earlier approximation, it was presumed that the electron density exhibited uniform distribution, yielding a homogeneous density. However, this approximation often diverged from experimental findings. Consequently, a new approach emerged, acknowledging the non-uniform and spatially varying nature of the localized electron density. Thus, the total energy of the electron system is now understood to be proportional to both the electron density $\rho(\vec{r})$ and its gradient $\nabla\rho(\vec{r})$, as depicted by the equation. [5]:

$$E_{XC}^{GGA}[\rho(\vec{r})] = \int d^3\vec{r}\rho(\vec{r})\varepsilon_{XC}\left[\rho\ (\vec{r}), \nabla\rho\ (\vec{r})\right]$$

6) Full-Potential Linearized Augmented Plane-wave Method (FP-LAPW)

Following the resolution of the exchange-correlation potential problem, the quest for wave functions as solutions to the Cohn-Sham equation became essential. Through extensive research, various approaches emerged, including the OPW method proposed by Herring theory in 1940 [26], the LMTO method [27], and the FP-LAPW method. It is important to highlight that the efficacy of these methods is contingent upon the quality of the effective potential employed.

6-1) The Plane Wave method (APW)

In the APW method, scientist Slater [10] implemented a strategy involving the division of crystal space into two segments, guided by the Muffin-Tin approximation [28]. Here, atoms were depicted as non-overlapping spheres with a radius of R0, encompassing core electrons, whereas the interstitial space between these spheres housed free electrons distanced from the atomic nuclei.

A graphical representation can illustrate the configuration of the elementary cell with atomic spheres and the interstitial region. According to Slater's approximation [10], the core electrons within the spheres encounter a spherical potential, whereas the potential remains constant within the interstitial region [3]. Therefore, the potential in these two regions can be expressed in the following form:

$$V(\vec{r}) = \begin{cases} V(r) r \leq R_0 \\ 0 r > R_0 \end{cases}$$

The behavior of electrons inside MT spheres is characterized by waves that are distinct from those in the interstitial region. In the interstitial region, plane waves are used to describe the behavior, whereas inside spheres, functions radials multiplied by spherical harmonics are employed. The two wave functions can be expressed as follows:

$$\varphi(\vec{r}) = \begin{cases} \sum_{l=0}^{\infty} \sum_{-m}^{m} A_{lm} U_l(r) Y_{lm}(r) \; r \leq R_0 \\ \frac{1}{\sqrt{\Omega}} \sum_{G} C_G \, e^{i(\vec{K}+\vec{G})\vec{r}} \; r > R_0 \end{cases}$$

Where , Ω: The cell volume

Y_{lm}: Spherical harmonics

A_{lm}: Development coefficients

U_l : The regular solution of the Schrödinger equation given by[6] :

$$\left(\frac{-d^2}{dr^2} + \frac{l(l+1)}{r^2} V(\vec{r})\right) r U_l = E_l U_l$$

Where E_l: An energy parameter.

6-2) The Linearized Augmented Plane Wave Method (LAPW)

A notable limitation of the APW method arises from its time-consuming computational procedure, largely attributable to the widespread use of the radial function Ul. It is difficult to define the radial function for each value of energy El. So that, Anderson [7] made improvements to the APW method [8]by using the Taylor expansion to write the radial functions U_l (r) in the following form:

$$U_l(r,E) = U_l(r,E_l) + (E_l - E)\left.\frac{dU_l(r,E)}{dE}\right|_{E=E_l} + O(E_l - E)^2$$

Where the term $\mathcal{O}(E - E_l)^2$represents the quadratic error.

After several simplifications, he has got the expression of potential inside and outside of Muffin-Tin balls as follows:

$$V(r) = \begin{cases} \sum_{lm}^{m} V_{lm}(r) Y_{lm} & r \le R_0 \\ \sum_{lm}^{m} V_k(r) e^{ikr} & r > R_0 \end{cases}$$

As well as the wave functions inside the spheres in terms of radial functions and their derivatives. Where the wave functions are written as follows [9,10]:

$$\Phi_{\vec{K}+\vec{G}}(\vec{r}) = \begin{cases} \sum_{lm} \left(A_{lm} U_l(r) + B_{lm} \dot{U}_l(r)\right) Y_{lm}(r) & r \le R_0 \\ \frac{1}{\sqrt{\Omega}} \sum_{G} C_G \, e^{i(\vec{K}+\vec{G})\vec{r}} & r > R_0 \end{cases}$$

Where :

$\vec{K}$: represents the wave vector.

$\vec{G}$: is the vector of the reciprocal lattice.

A_{lm}:: are coefficients corresponding to the function U_l.

B_{lm}: are coefficients corresponding to the function U_l.

We can determine the coefficients A_{lm} and B_{lm}, for each wave vector, and for each atom by applying the conditions of continuity of the basic functions in the vicinity of the limit

of the spheres. After some simplifications we find the coefficient formula A_{lm} and B_{lm} in the following forms:

$$A_{lm} = \frac{4\pi {r_0}^2 i^L}{\sqrt{\Omega}} {Y^*}_{lm}(K+G) a_l(K+G)$$

$$B_{lm} = \frac{4\pi {r_0}^2 i^L}{\sqrt{\Omega}} {Y^*}_{lm}(K+G) b_l(K+G)$$

7) Simulation Code WIEN2K

The Institute of Materials Chemistry in Vienna has harnessed technological advancements, particularly in programming languages, to create the wien2k program package [34], a significant achievement in computational materials science. This esteemed program is renowned for its utility in investigating the properties of solid materials. It encompasses a plethora of subprograms coded in the Fortran language, with the latest iterations boasting sophisticated algorithms designed to adeptly translate crystal system equations rooted in density functional theory (DFT). These cutting-edge algorithms leverage the full potential linearized augmented plane wave (FP-LAPW) method to meticulously compute and analyze compound properties. Through the utilization of wien2k, researchers can delve deeper into the intricate nature of materials, unveiling valuable insights into their structural and electronic characteristics. [3].

The most important subprograms and its role in the Wien2k program are shown in the diagram shown in Figure I.3 which are organized as follows:[4]:

NN : This program computes the distances between adjacent neighbors within a set limit, aiding in the calculation of the atomic sphere's radius.

- ✓ **SGROUP** :determines the space group of the compound.
- ✓ **SYMMETRY** :is a program that defines the symmetry number and space group symmetry operations of our structure.
- ✓ **LSTART** :calculates electron densities in free atoms and show how different orbitals will be treated in band structure calculations.
- ✓ **KGEN** : generates a mesh of K points in the irreducible part of the first Brillouin zone (B.Z). We specify the number of K points in the whole 1stB.Z.

- ✓ **DSTART** :produces an initial density for the SCF cycle (self-consistent cycle) by a superposition of atomic densities produced in the LSTART subprogram.

After the last subprogram ; we enter a loop of SFC calculations and therefore we shall reach five steps :

- ✓ **LAPW0 (POTENTIAL)** :uses the total electron density to calculate the coulombien and exchange potential (Hartree-Fock potential). In addition to that, it divides the space into a MT (muffin-tin) sphere and an interstitial region.
- ✓ **LAPW1 (BANDS) :** calculate eigenvalues and wave functions for valence electrons from solving the equation (III.1).
- ✓ **LAPW2 (RHO)** : calculate the valence electron densities obtained in the step LAPW0.
- ✓ **LCORE** :calculates eigenvalues and wave functions to obtain core electron densities.
- ✓ **MIXER** : calculate the new density by mixing.

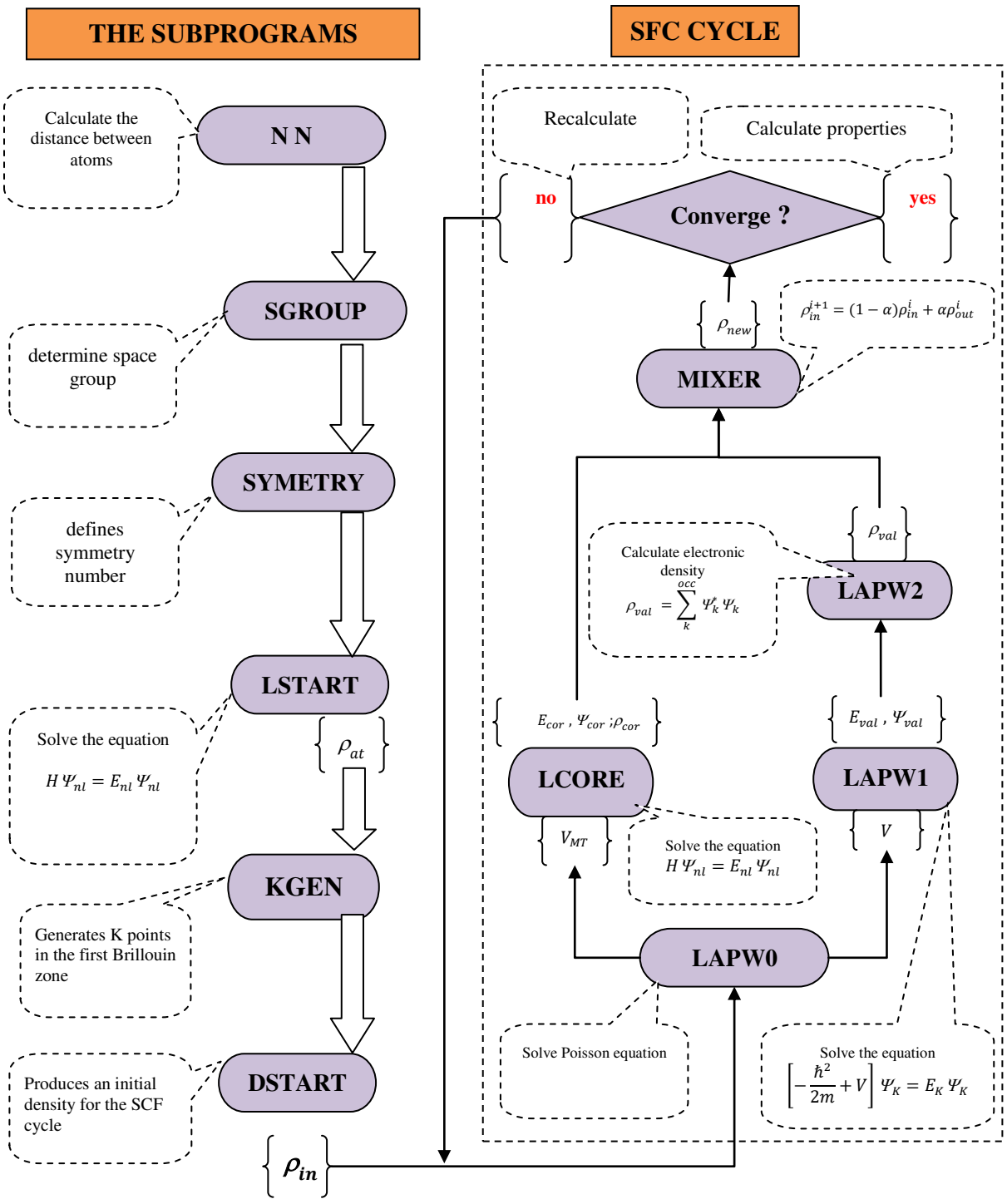

Figure I. 3 : The flowchart of program code Wien2k [4].

8) References

[1] E.SCHROEDINGER,QuantizationasaProblemofProperValues(PartI),Ann.Phys. (1926). https://ci.nii.ac.jp/naid/10022177951/en/.

[2] S.S. Essaoud, M. Imadalou, D.E. Medjadi, Microscopic Study of Correlations in Finite FermionicSystemsbyBreakingtheAxialSymmetry, IntJMod. TheoPhys.5(2016)8– 21.

[3] S.SaadEssaoud,Lescomposésàbasedemanganèse:investigationthéoriquedes propriétés structurales électroniques et magnétiques, 2020. https://doi.org/10.13140/RG.2.2.30742.68169.

[4] S.SaadEssaoud,Etudemicroscopiquedescorrélationsdanslessystèmesfermioniques finisenbrisantlasymétrieaxiale,2013.https://doi.org/10.13140/RG.2.2.19283.71203 .

[5] M.Born,R.Oppenheimer,ZurQuantentheoriederMolekeln,Ann.Phys.389(1927) 457–484. https://doi.org/10.1002/andp.19273892002.

[6] D.R.Hartree,Thewavemechanicsofanatomwithanon-coulombcentralfield.PartII. Someresultsanddiscussion,in:Math.Proc.Camb.Philos. Soc.,Cambridge University Press, 1928: pp. 111–132.

[7] D.R.Hartree,Thewavemechanicsofanatomwithanon-coulombcentralfield.partiii. term values and intensities in series in optical spectra, in: Math. Proc. Camb. Philos. Soc., Cambridge University Press, 1928: pp. 426–437.

[8] G.Shadmon,I.Kelson,Multi-determinantalhartree-focktheory,Nucl.Phys.A.241 (1975) 407–428. https://doi.org/10.1016/0375-9474(75)90395-4.

[9] V.Fock,„Selfconsistentfield“mitAustauschfürNatrium,Z.FürPhys.62(1930)795–805.

[10] J.C.Slater,DampedElectronWavesinCrystals,Phys.Rev.51(1937)840–846. https://doi.org/10.1103/physrev.51.840.

[11] P.A.M.Dirac,NoteonExchangePhenomenaintheThomasAtom,Math.Proc.Camb. Philos. Soc. 26 (1930) 376–385. https://doi.org/10.1017/S0305004100016108.

[12] J.C.Slater,ASimplificationoftheHartree-FockMethod, Phys.Rev. 81(1951)385–390. https://doi.org/10.1103/PhysRev.81.385.

[13] P.Hohenberg,W.Kohn,InhomogeneousElectronGas,Phys.Rev.136(1964)B864–B871. https://doi.org/10.1103/physrev.136.b864.

[14] L.H.Thomas,Thecalculationofatomicfields,Math. Proc.Camb.Philos.Soc.23 (1927) 542. https://doi.org/10.1017/s0305004100011683.

[15] E.Fermi,EinestatistischeMethodezurBestimmungeinigerEigenschaftendesAtoms und ihre Anwendung auf die Theorie des periodischen Systems der Elemente, Z. Für Phys. 48 (1928) 73–79.

Thesis,Masterللمركب CsVO3ل.مروة,دراسةالخواصالكهروحراريةوالترموديناميكية

[16]2021.BOUDIAF-M'SILA,MOHAMEDUNIVERSITE

[17]2021.BOUDIAF-آ.قريشي,دراسةنظريةللخواصالبنيوية،االلكترونيةوالضوئيةللمركبين Masterk3MgF,AgMgF M'SILA,MOHAMEDUNIVERSITEThesis,

[18] R.M.Dreizler,E.K.U.Gross,DensityFunctionalTheory,(1990) . https://doi.org/10.1007/978-3-642-86105-5.

[19] R.Stowasser,R.Hoffmann,WhatdotheKohn-Shamorbitalsandeigenvaluesmean?,J. Am. Chem. Soc. 121 (1999) 3414–3420.

[20] A.Seidl,A.Görling,P.Vogl,J.A.Majewski,M.Levy,GeneralizedKohn-Sham schemes and the band-gap problem, Phys. Rev. B. 53 (1996) 3764.

[21] C.Fiolhais,F.Nogueira,M.A.Marques,Aprimerindensityfunctionaltheory,Springer Science & Business Media, 2003.

[22] F.M.Bickelhaupt,E.J.Baerends,Kohn-Shamdensityfunctionaltheory:predictingand understanding chemistry, Rev. Comput. Chem. 15 (2000) 1–86.

[23] J.A.Pople,P.M.Gill,B.G.Johnson,Kohn—Shamdensity-functionaltheorywithina finite basis set, Chem. Phys. Lett. 199 (1992) 557–560.

[24] W.Kohn,L.J.Sham,Self-ConsistentEquationsIncludingExchangeandCorrelation Effects, Phys. Rev. 140 (1965) A1133–A1138. https://doi.org/10.1103/physrev.140.a1133.

[25] D.M.Ceperley,B.J.Alder,GroundStateoftheElectronGasbyaStochasticMethod, Phys. Rev. Lett. 45 (1980) 566–569. https://doi.org/10.1103/physrevlett.45.566.

[26] C.Herring,Anewmethodforcalculatingwavefunctionsincrystals,Phys.Rev.57 (1940) 1169.

[27] H.L. Skriver, The LMTO Method: Muffin-Tin Orbitals and Electronic Structure,

Springer-Verlag,BerlinHeidelberg,1984.https://doi.org/10.1007/978-3-642-81844-8.

[28] O.K.Andersen,T.Saha-Dasgupta,Muffin-tinorbitalsofarbitraryorder,Phys.Rev.B. 62 (2000) R16219.

[29] D D Koelling and G O Arbman, Use of energyderivative of the radial solution in an augmentedplanewavemethod:applicationtocopper,J.Phys.FMet.Phys.5(1975) 2041.

[30] O.K.Andersen,Linearmethodsinbandtheory,Phys.Rev.B.12(1975)3060–3083. https://doi.org/10.1103/physrevb.12.3060.

[31] M.Petersen,F.Wagner,L.Hufnagel,M.Scheffler,P.Blaha,K.Schwarz,Improvingthe efficiency of FP-LAPW calculations, Comput. Phys. Commun. 126 (2000) 294–309.

[32] D.R.Hamann,SemiconductorChargeDensitieswithHard-CoreandSoft-Core Pseudopotentials, Phys. Rev. Lett. 42 (1979) 662–665. https://doi.org/10.1103/physrevlett.42.662.

[33] M.Weinert,SolutionofPoisson'sequation:BeyondEwald-typemethods,J.Math.Phys. 22 (1981) 2433–2439. https://doi.org/10.1063/1.524800.

[34] P.Blaha,K.Schwarz,G. Madsen,D.Kvasnicka,J.Luitz,Wien2k, (2001).

CHAPTER 02/ DISCUSSION OF OBTAINED RESULTS

Sommaire

1) Introduction

Building upon the theoretical framework discussed earlier, our investigation commenced by exploring the structural characteristics of SrSnO3. Employing advanced computational tools such as Wien2k Density Functional Theory (DFT) and Full-Potential Linearized Augmented Plane Wave (FPLAPW) methods, we meticulously computed essential parameters including lattice parameters, the compressibility coefficient, and its first derivative. Subsequently, we delved into the compound's electronic behavior, utilizing sophisticated analysis techniques to dissect band structure curves and density of states. Lastly, our inquiry extended to the calculation of the compound's thermal and thermoelectric properties, thereby providing a comprehensive understanding of its multifaceted nature.

2) Accountdetails:

The computations in this study utilized the full-potential linearized augmented plane wave (FP-LAPW) method implemented in the Wien2K simulation program, which relies on density functional theory (DFT) [1–13]. To treat the exchange-correlation effects, the generalized gradient approximation (GGA) [14, 15]. These techniques were instrumental in estimating the compound's structural, electronic, and optical properties.

Applying the muffin-tin (MT) approximation, we partitioned the space into two distinct regions[16]. In the first region, atoms were treated as spheres with muffin-tin radii, accommodating all inner electrons ('core electrons') without overlap. For the compound, the 'Sr,' 'O,' and 'Sn' atoms were assigned half radii values of 2.2 a.u, 1.4 a.u, and 2.25 a.u, respectively, with a maximum angular momentum of lmax = 10.

The second region, representing the intermediate space, was characterized by plane wave functions with a cutoff parameter RMTKmax, where RMT is the average half radius of the muffin-tin spheres, and Kmax is the maximum value of the wave vector for the reciprocal lattice.

The optimal cutoff parameter was determined as RMTKmax = 8, with a total of kpoints1000=. The electronic configurations for the constituent atoms were assigned as follows: Sr: [Kr] 5s2, O: [He] 2s2 2p4, and Sn: [Kr] 4d10 5s25p2.we employed a quasi harmonic Debye model integrated into the GIBBS2 program to investigate the impact of pressure and temperature on the thermal properties. Additionally, we utilized a Boltzmann transport equation model integrated in BoltzTrap code to study the thermoelectric properties

3) The obtained results

3-1) structural Properties

SrSnO3 adopts a cubic crystal structure within the space group Pm-3m. The primitive unit cell, illustrated in Figure II.1 using the VESTA program[17–20], comprises 5 atoms distributed across distinct Wyckoff positions. Specifically, Sr occupies position (0 0 0), Sn resides at (0.5 0.5 0.5), and oxygen atoms are found at (0.5 0.5 0), (0.5 0 0.5), and (0 0.5 0.5). This arrangement provides a foundational understanding of the compound's atomic configuration, facilitating further analysis of its properties and behavior.

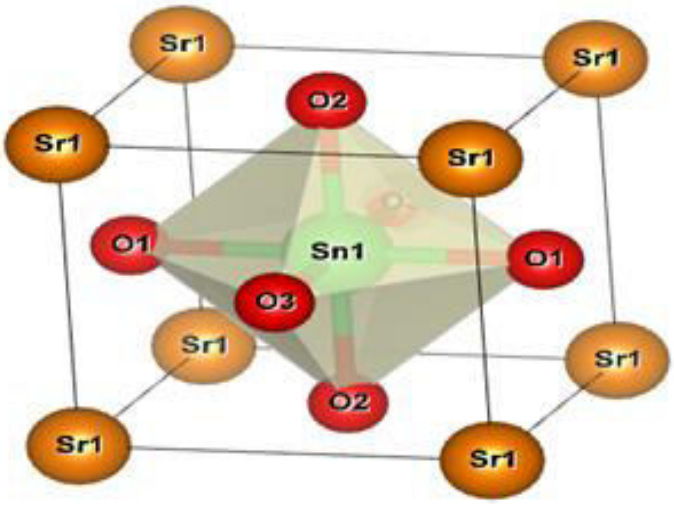

Figure (II.1): Crystal structure of the compound $SrSnO_3$ (achieved using the VESTA program).

In our analysis of the structural properties of SrSnO3, we began by calculating the variations in total energy of the primitive cell at different volumes, employing the generalized gradient approximation (GGA). Subsequently, we depicted the relationship between total energy changes and volume by plotting a curve, utilizing the Murnaghan equation [21]. This equation is defined as follows:

$$E(V) = E_0 + \frac{B}{B'(B'-1)}\left[V\left(\frac{V_0}{V}\right)^{B'} - V_0\right] + \frac{B}{B'}(V - V_0)$$

Where:

- V_0**:** represents the volume of the cell at equilibrium.
- E_0**:** represents the total energy of the primitive cell in equilibrium.
- B**:** is the bulk modulus.
- **B':** is the derivative of the bulk modulus with respect to pressure

This mathematical representation allowed us to characterize the behavior of SrSnO3 under varying volumes, providing insights into its structural stability and elasticity properties. The curves depicted in Figure (II.2) enabled us to identify the volume associated with the minimum energy state. Subsequently, we derived the lattice constant

a (in Ångströms) and the bulk modulus from this minimum energy volume. To contextualize our findings, we compared these calculated values with both experimental and theoretical results, as summarized in Table (II.1). Remarkably, our results exhibited a high degree of consistency with those obtained in prior studies, further validating the accuracy of our computational approach and reinforcing the understanding of SrSnO3's structural characteristics.

Compound Name	Calculated Structural Properties	Our results	Other results
	Cell parameter a (Å)	4.1610	4.034
	Bulk modulus B (GPa)	57.5176	

$SrSnO_3$	B' (GPa)	2.2940	
	V_0	486.1626	

Table (II.1): Calculated structural properties values for the compound $SrSnO_3$ using GGA approximations.

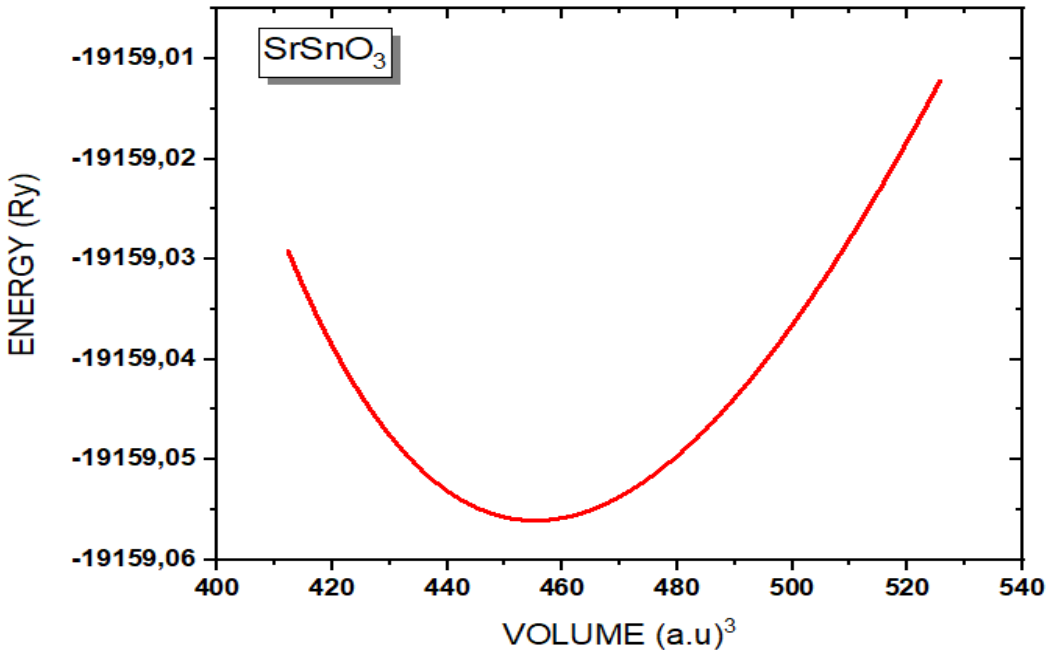

Figure (II.2): Total energy variations of the compound $SrSnO_3$ as a function of volume changes.

3-2) ElectronicProperties

Studying electronic properties is crucial, as it enables us to select the appropriate electrical or electronic application for a given material. By understanding the compound's electronic properties, we can make informed decisions about its potential uses. To achieve this, we conducted an in-depth analysis of the compound's energy bands to determine its electronic behavior, identifying whether it is an insulator, conductor, or semiconductor. Furthermore, we examined the density of states to pinpoint the atomic orbitals influencing each band. This detailed analysis aids in understanding the formation of atomic bonds and the overall behavior of the material at the atomic level, providing valuable insights into its potential applications.

In this section, we will study the electronic properties by analyzing the energy band structure curves. Then, we will analyze the partial and total density of states curves for the SrSnO3 compound.

3-2-1) Band-Structure spectra

To assess the electronic behavior of SrSnO3 under equilibrium conditions, we analyzed the band structures generated by GGA method. Our findings, illustrated that the top of the valence band and the bottom of the conduction band reside at distinct high symmetry points, confirming the compound's indirect band gap type (M−Γ) with 1.21 eV calculated using GGA approximation.

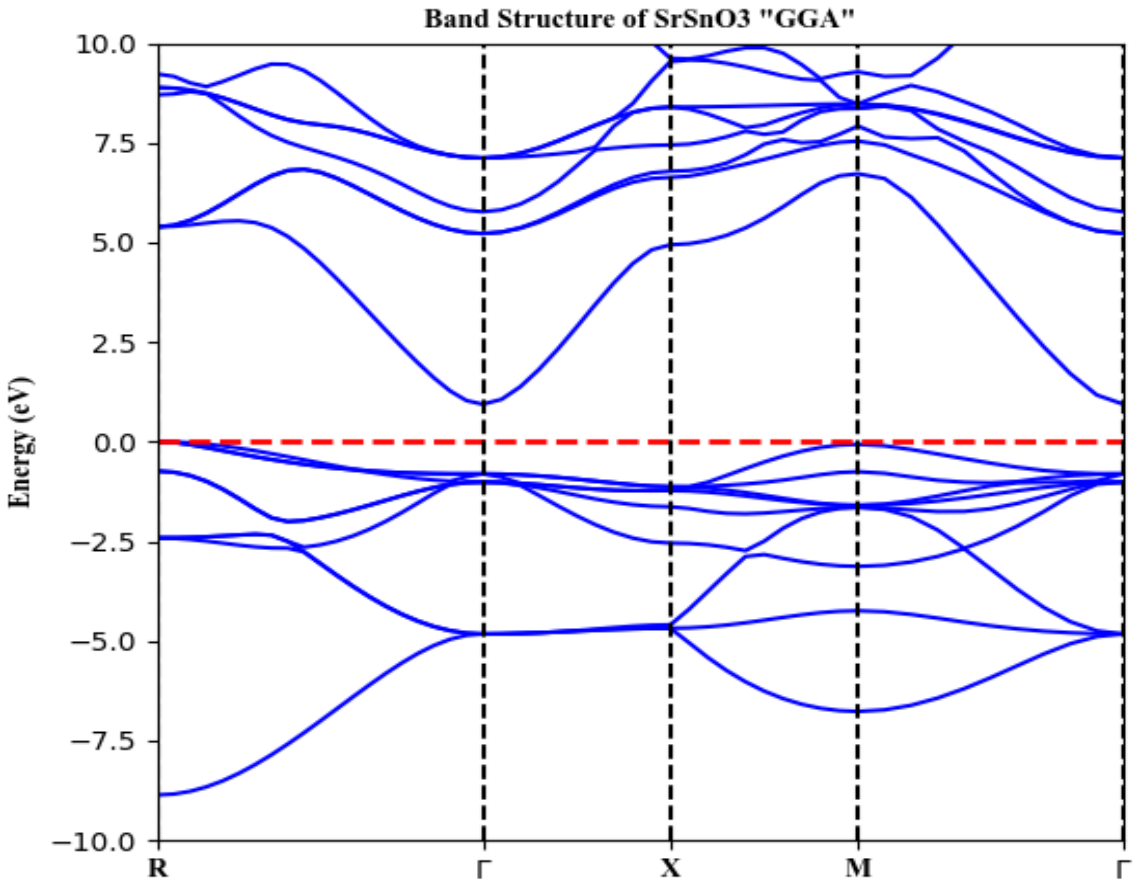

Figure (II.3): band structure spectra for the compound SrSnO3 calculated using GGA approximation.

3-2-2) Total Density of States (TDOS) and Partial Density of States (PDOS)

In this section, we will analyze the curves representing the total density of states distribution as well as the partial density of states. This analysis aims to determine which atomic orbitals' electrons contributed to forming the energy bands discussed earlier.

Figure (II.4) provides insight into the distribution of both the total and partial density of states for SrSnO3, calculated using the GGA approximation. Here are the key observations:

- Total Density of States:

❖ Notably, there are no values near the Fermi level, confirming the compound's semiconducting behavior.

- Contributions of Atomic Orbitals:

❖ Valence Band:

❖ Between -8 eV and -6 eV: A pronounced contribution from the 's' orbitals of Sn atoms is evident.

❖ Moving from -6 eV to 0 eV: We observe a weaker involvement from the 'p' and 'd' orbitals of Sn atoms, along with the 'p' orbitals of O atoms, indicating a varied orbital influence.

❖ Conduction Band:

❖ In the range of 1 eV to 6 eV: There's a minor but noticeable contribution from the 's' orbitals of Sn atoms.

❖ Within the interval from 6 eV to 9 eV: Both 's' and 'p' orbitals of Sr atoms contribute slightly, suggesting their role in the material's conductive properties.

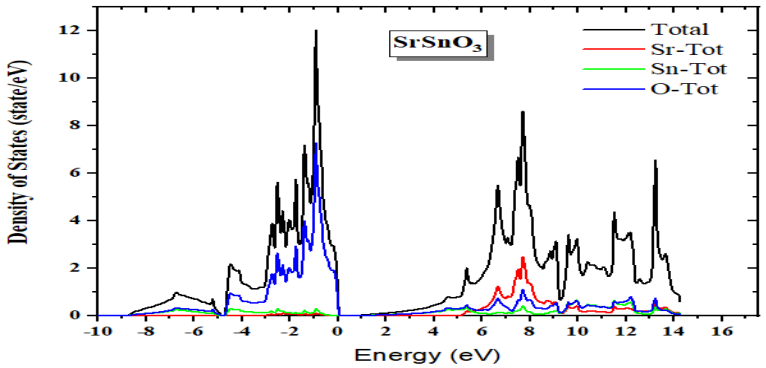
SrSnO3
Total
Sr-Tot
Sn-Tot
O-Tot
Density of States (state/eV)
Energy (eV)

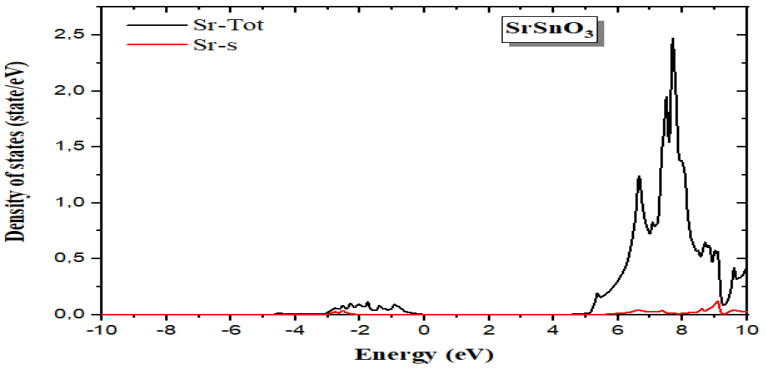
SrSnO3
Sr-Tot
Sr-s
Density of states (state/eV)
Energy (eV)

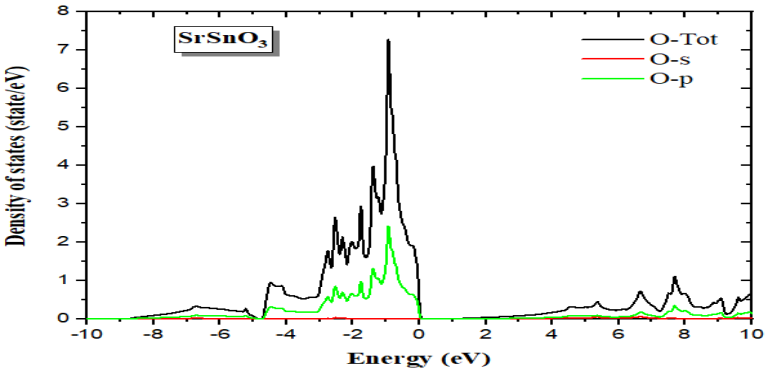
SrSnO3
O-Tot
O-s
O-p
Density of states (state/eV)
Energy (eV)

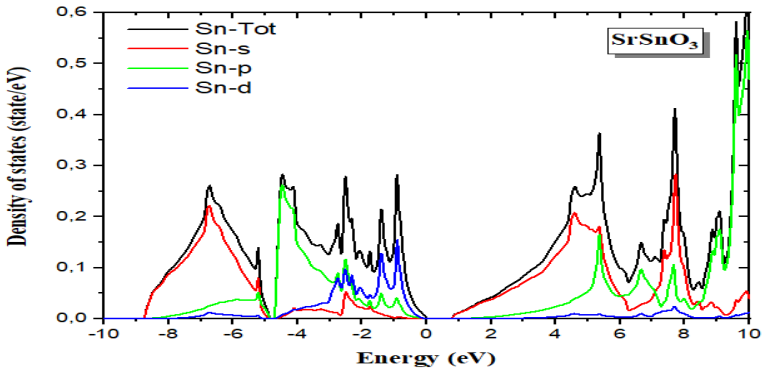

Figure (II.4): Electronic properties of the compound $SrSnO_3$ (Total and Partial Density of States)

3-3) ThermodynamicProperties (Thermal)

3-3-1) Debye model

The first-principle calculation utilizing the WIEN2k program was conducted at zero temperature. This involved neglecting the vibrational aspects of the atoms within the Hamiltonian equation of the crystal system, achieved through the application of the Born-Oppenheimer approximation[49]. While this approach provides valuable insights into the electronic properties of SrSnO3, it's crucial to recognize the significant impact of temperature and pressure on the compound's properties. Future investigations should consider incorporating thermal and pressure effects to comprehensively understand SrSnO3's behavior under varying conditions.. Here, we have studied the effect of temperature on thermodynamic variables by using the quasi-harmonic model [50] as implemented in GIBBS2 code [25,26]. The function controlling the phase stability of a solid at a given pressure and temperature is the Gibbs free energy given by:

$$G^*(x,V;P,T) = E_{sta}(x,V) + PV + A^*_{vib}(x,V;T) + F^*_{el}(x,V;T) \quad (9)$$

Where E is the total energy, PV corresponds to the hydrostatic condition, A^*_{vib} and $F^*_{el}$are the non-equilibrium vibrational and electronic free energies, respectively. Debye's model is used to describe the vibrational energy A^*_{vib}in terms of the density of phonon states (the vibrational density of states) g(ω):

$$A^*_{vib} = \int_0^{\infty} \left[\frac{\omega}{2} + k_B T \, Ln\,(1 - e^{-\frac{\omega}{k_B T}})\right] g(\omega) d\omega \quad (10)$$

$$F^*(x, V; T) = E_{sta}(x, V) + A^*_{vib}(x, V; T) (11)$$

in this equation, n is the number of atoms per unit volume, D (θ / T) represents the Debye integral, which is given by:

$$D(x) = \frac{3}{x^3}\int_0^x \frac{y^3 e^{-y}}{1-e^{-y}}\, dy (12)$$

The equilibrium state (for pressure (P) and a temperature (T) given) is obtained by the minimization of:

$$\left(\frac{\partial G^*(V,P,T)}{\partial V}\right)_{P,T} = 0 (13)$$

Resolving the last equation makes it easy to express the other thermal quantities in particular: entropy (S), the heat capacity at constant volume (C_v), and the coefficient of thermal expansion, which are given:

$$S = -3nk_B \ln\left(1 - e^{-\Theta_D/T}\right) + 4nk_B D(\Theta_D/T) (14)$$

$$C_v = 12nk_B D(\Theta_D/T) - \frac{9nk_B\Theta_D/T}{e^{\Theta_D/T}-1} (15)$$

$$\alpha = -\frac{1}{V}\left(\frac{\partial V}{\partial T}\right)_P = \frac{\gamma C_v}{V B_T} (16)$$

In this section, we've dedicated our efforts to delve into various thermal properties of SrSnO3. Our exploration encompasses crucial parameters like heat capacity at constant pressure or volume, thermal expansion coefficient, entropy, and compressibility. These properties are investigated under the influence of two significant natural factors: hydrostatic pressure and temperature.

Examining the pressure exerted on the substance, our analysis spans across three distinct levels: 0 GPa, 5 GPa, and 10 GPa. Concurrently, we explore the compound's response to temperature variations within the range of 0 to 1000 Kelvin. By comprehensively studying these thermal properties under diverse conditions, we aim to gain a deeper understanding of SrSnO3's behavior in real-world scenarios.

3-3-2) HeatCapacities

The heat capacity of a solid indicates how much heat it absorbs when its temperature rises by one degree. For metals, this property is crucial as it reflects their ability to absorb thermal energy, which depends on factors like the material's degrees of freedom and available vibrational modes. Our study examined the impact of temperature and pressure on the heat capacity of SrSnO3, conducting calculations at pressures of 0 GPa, 5 GPa, and 10 GPa. Our findings[28,29],

illustrated in figure (II.5), reveal that at constant volume (Cv), the heat capacity increases rapidly with temperature, following a cubic relationship (T^3) at low temperatures. This increase slows down at higher temperatures, converging toward a limit according to the Dulong-Petit law[36]. Similar trends were observed for heat capacity at constant pressure (Cp), indicating an accelerated increase at low temperatures and a slower rise at higher temperatures.

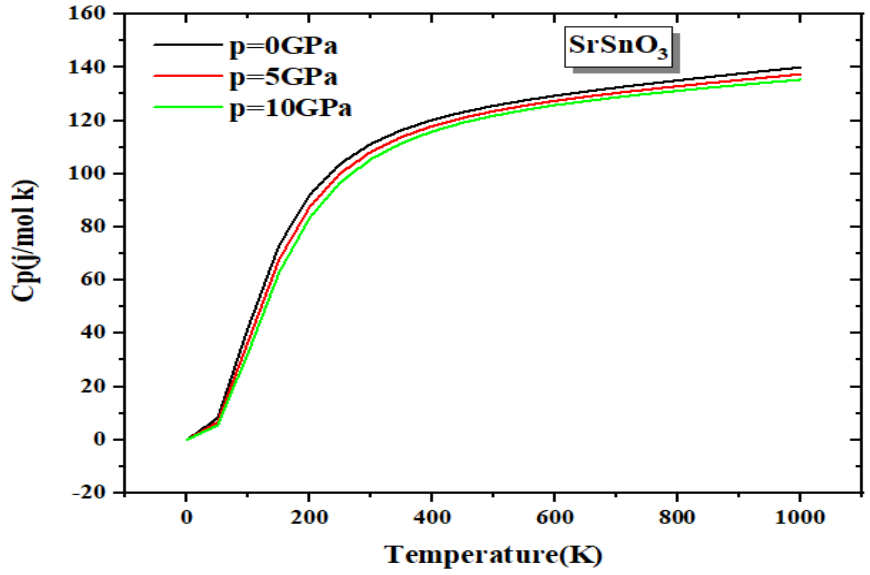

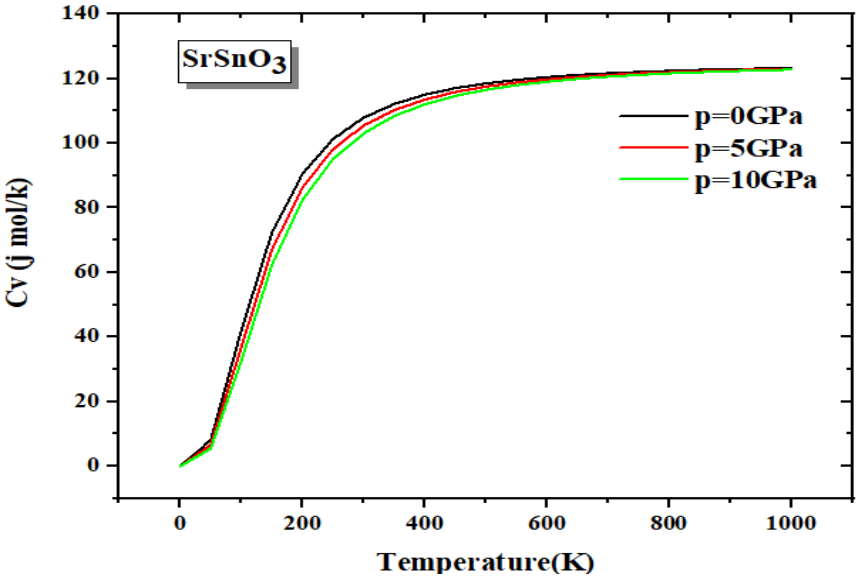

Figure (II.5): Changes in the heat capacities ($C_p$and C_v) of the compound $SrSnO_3$ as a function of temperature.

3-3-3) Entropy

Entropy, a complex concept with diverse applications, is particularly relevant in thermal studies. It operates at two levels:

1. Microscopic: It quantifies the disorder in a system, expressed as S = k ln Ω, where Ω denotes the number of possible arrangements or states the compound can assume.

2. Macroscopic: It represents the internal energy of the substance, which cannot be utilized for work[28,29].

The value of entropy is intricately linked to a substance's internal structure and is influenced by various factors, leading to alterations such as atomic vibrations and electron transitions.

In our study, we explored entropy changes under different temperatures (0 GPa, 5 GPa, and 10 GPa). We observed a direct correlation between entropy and temperature changes, indicating increased disorder in SrSnO3 as temperature rises, as depicted in figure (II.6). This rise in temperature leads to the compound adopting new configurations due to atomic vibrations, thus increasing its diversity.

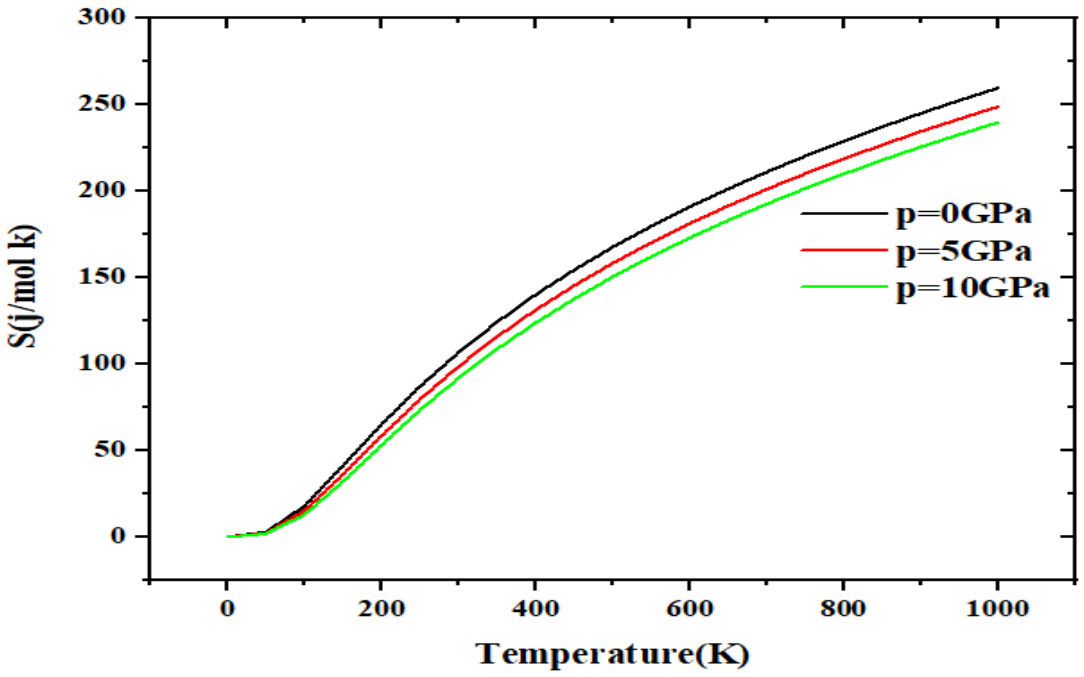

Figure (II.6): Changes in entropy (S) of the compound $SrSnO_3$ as a function of temperature.

3-3-4) Thermal Expansion Coefficient

The thermal behavior of solid materials in electronic devices is critical, particularly for those generating significant heat. A key thermal property, the thermal expansion coefficient, is vital because material expansion can lead to device fracturing or exert pressure on internal components, potentially affecting electronic properties. Thermal expansion occurs as thermal energy increases atomic vibrations, causing atoms to move from their equilibrium positions. The thermal expansion coefficient depends on factors like bond nature, material density, and atomic arrangement[28,29]. For SrSnO3, calculated using the GIBBS2 program up to 1000 Kelvin under constant pressures, the resulting curve (shown in figure 7.II) reveals rapid expansion at low temperatures (below 200 Kelvin) and a slower increase at higher temperatures.

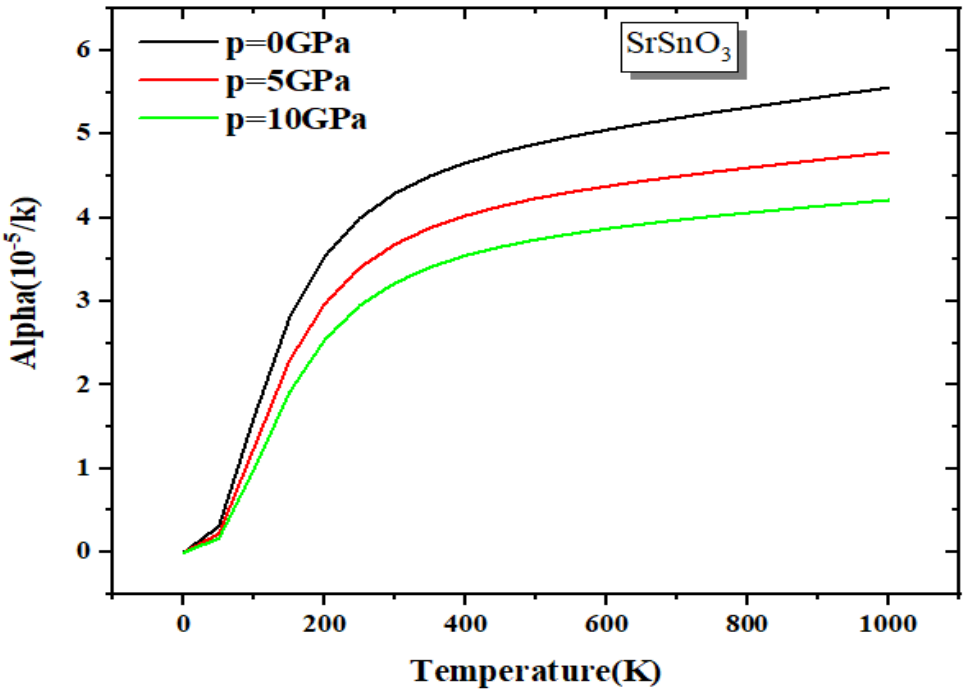

Figure (II.7): Changes in the thermal expansion coefficient (α) of the compound $SrSnO_3$ as a function of temperature.

3-4) Thermoelectric Properties

The thermoelectric properties, including Seebeck coefficient, electrical conductivity and thermal conductivity, of the considered compounds were calculated from the energy bands using the Boltzmann transport theory with the rigid band approach (RBA) [42–44]and the constant scattering time approximation (CRTA) as implemented in the BoltzTrap program [45]. Based on this approach, the Seebeck coefficient (S) and the electrical conductivity (σ) as functions of absolute temperature T and chemical potential μ can be calculated from the band structure calculation by integrating the transport distribution tensor $\bar{\sigma}_{\alpha\beta}(\varepsilon)$ as follows [45]:

$$\sigma_{\alpha\beta}(T,\mu)=\frac{1}{\Omega}\int\bar{\sigma}_{\alpha\beta}(\varepsilon)\left[-\frac{\partial f_0(T,\varepsilon,\mu)}{\partial E}\right]d\varepsilon \quad (1);$$

$$S_{\alpha\beta}(T,\mu)=\frac{1}{eT\Omega\sigma_{\alpha\beta}(T,\mu)}\int\bar{\sigma}_{\alpha\beta}(\varepsilon)(\varepsilon-\mu)\left[-\frac{\partial f_0(T,\varepsilon,\mu)}{\partial\varepsilon}\right]d\varepsilon \quad (2)$$

where α and β are tensor indices, Ω is the volume of the unit cell, f_0 is the Fermi-Dirac distribution function and e is the electron charge. The essential part of σ and S is the transport distribution function tensor $\bar{\sigma}_{\alpha\beta}(E)$, which contains the system dependent information, defined as:

$\bar{\sigma}_{\alpha\beta}(\varepsilon)=\frac{e^2}{N}\sum_{i,k}\tau_{i,k}\upsilon_\alpha(i,k)\upsilon_\beta(i,k)\frac{\delta(\varepsilon-\varepsilon_{i,k})}{\delta\varepsilon}$ (3), where N is the number of k-points, i is the band index, $\boldsymbol{k}$ is the wave vector and $\upsilon_\alpha(i,k)$ (α = x, y, z) is the αth component of the group velocity v(i, k) of charge-carriers, which can be obtained directly from the band structure calculation as: $\upsilon_\alpha(i,k)=\frac{1}{\hbar}\frac{\partial E_{i,k}}{\partial k_\alpha}$, where $\hbar$ is the reduced Planck constant. The wave vector dependent relaxation time ($\tau_{i,k}$) appearing in the expression of $\bar{\sigma}_{\alpha\beta}(E)$ is difficult to be determined from first-principles calculations and hence eq. 3 is solved under constant relaxation time approximation (RTA).

Having examined the thermal properties of SrSnO3 under heat, our focus now shifts to understanding how temperature variations affect the material's electrons. Research, as summarized in the article "Thermoelectric Devices: Principle and Future Trends" by Abd al-Muttalib and al-Qadri [37], indicates that materials with semi-metallic electronic behavior demonstrate excellent thermoelectric properties. Consequently, they are highly suitable for applications in thermoelectric devices such as generators, sensors, and motors. Since SrSnO3 exhibits semi-metallic behavior, we aim to investigate its thermoelectric properties, including the Seebeck coefficient, thermal conductivity, electrical conductivity, and the ZT factor.[29].

3-4-1) Seebeck Coefficient

he Seebeck coefficient, as an intrinsic electrical property of solid-state materials, describes the electric potential difference (voltage) between the ends of a material subjected to different temperatures. This voltage difference arises due to the movement of electrons in response to temperature gradient, from hotter regions to cooler ones [29, 38].

Figure (8.II) illustrates the changes in the Seebeck coefficient of the compound $SrSnO_3$ as a function of temperature. From this figure, we observed the following points:

1. The Seebeck coefficient values are high at an intermediate temperature, around 300 Kelvin, whereas they are low at temperatures exceeding 600 Kelvin.

2. The maximum Seebeck coefficient occurs when the relative chemical potential (relative to the Fermi level) is confined between 0 and 1 electron-volts, and it diminishes outside this range.

3. The maximum value of the Seebeck coefficient recorded at temperatures around 300 Kelvin is approximately 0.0009 mV/K.

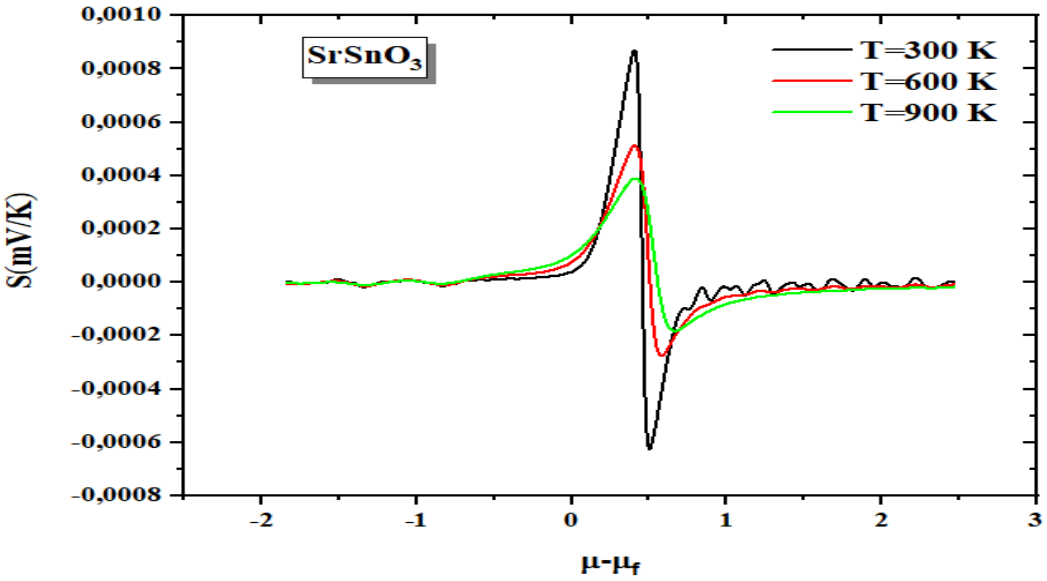

Figure (II.8): Changes in the Seebeck coefficient of the compound $SrSnO_3$ at different temperatures as a function of chemical potential variations.

3-4-2) ElectricalConductivity

Electrical conductivity, or electrical transport, in solid materials is also an important feature, representing the material's ability to conduct and carry electrical current, i.e., allowing free electrons to pass through it. Electrical conductivity is related to the internal structure of materials, their electronic behavior, and external factors such as temperature, which leads to atomic vibrations and thus interactions between electrons (charge carriers) and phonons [29, 38].

Figure (II.9) depicts the changes in electrical conductivity as a function of temperature for the studied compound. From this figure, we observed the following points:

1. Electrical conductivity reaches its maximum within the chemical potential range between (-1.5; -0.5).
2. As the temperature increases within this chemical potential range (-1.5; -0.5), the electrical conductivity decreases. This is because the resistance increases due to the increased vibrations of the crystal lattice atoms.

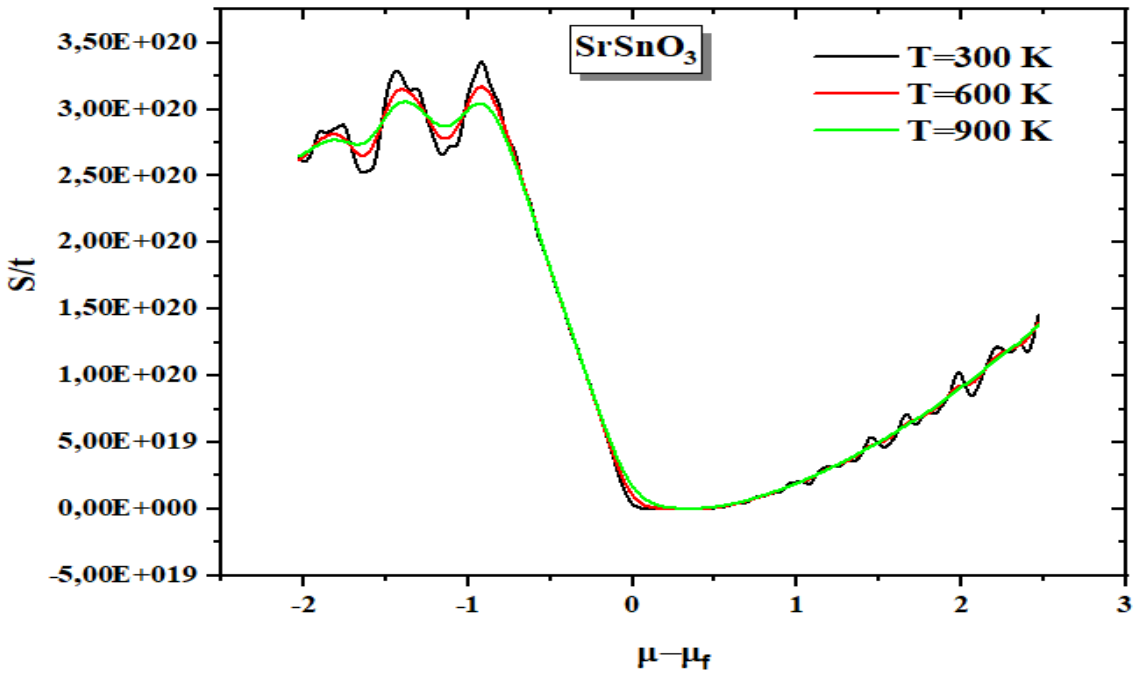

Figure (II.9): Electrical conductivity of the compound $SrSnO_3$ at different temperatures as a function of chemical potential variations.

3-4-3) Electronic Thermal Conductivity

Electrons also contribute to electrical conductivity, as there is a portion of heat transferred with the electrons in addition to the heat transferred through atomic vibrations (via the dispersion of phonons in the crystal lattice) [29,38]. Figure (II.10) illustrates the changes in electronic thermal conductivity as a function of temperature for the studied compound, from which we recorded the following points:

- We notice that as the temperature increases, the value of electronic thermal conductivity increases.
- We notice that thermal conductivity exhibits behavior similar to electrical conductivity for all compounds. This confirms that electron transfer contributes to heat transfer, as thermal conductivity is proportional to electrical conductivity, following the relationship given by the Wiedemann-Franz law:

$K_e = L\sigma T$ (where L is the Lorentz number)

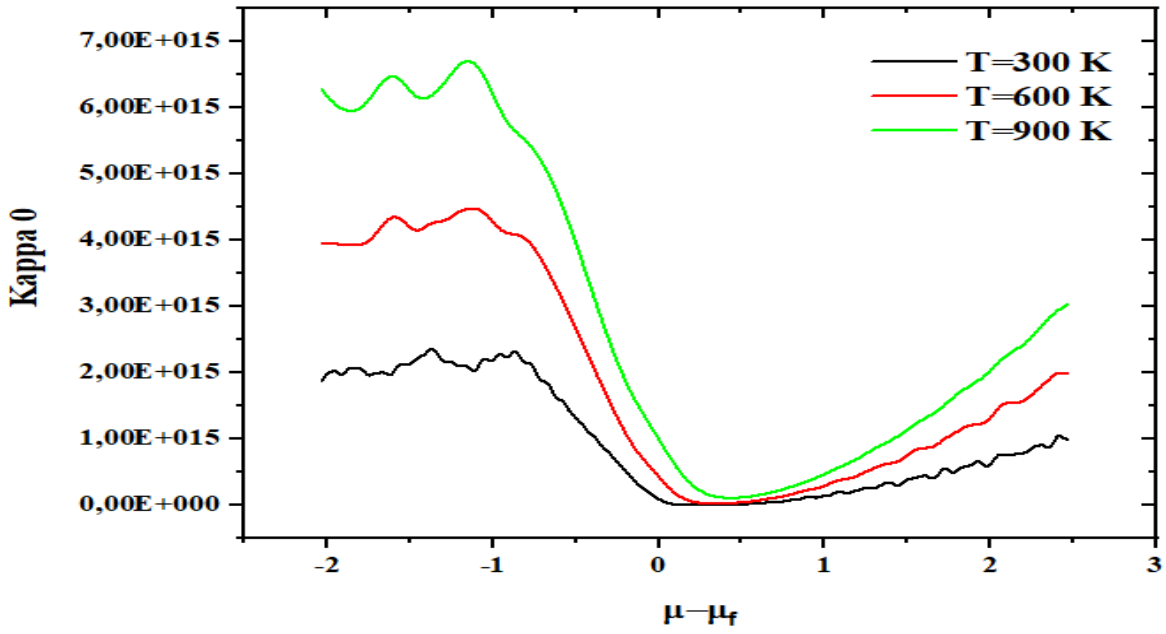

Figure (II.10): Electronic thermal conductivity of the compound $SrSnO_3$ at different temperatures as a function of changes in chemical composition.

3-4-4) ZT coefficient

The optimal selection of materials in terms of their thermoelectric efficiency is at the core of much theoretical and experimental research. The effective performance of thermoelectric materials is evaluated through the dimensionless figure of merit ZT, which is given by the following expression:

$$ZT = \frac{S^2 T\sigma}{\kappa}$$

Where S is the Seebeck coefficient, σ is the electrical conductivity, κ is the total thermal conductivity, and T is the absolute temperature. Therefore, we can achieve high thermoelectric performance when the materials have high Seebeck coefficient, high electrical conductivity, and low thermal conductivity[29]. The changes in the ZTcoefficient at different temperatures due to the variation of chemical doping are illustrated in Figure (11.II). It can be observed from this figure that the values of this coefficient are maximized when the chemical doping is confined within the range of -1 to 1 electron-volt for all temperatures. Outside of this range, the value of this coefficient becomes nearly zero or zero altogether for all temperatures.

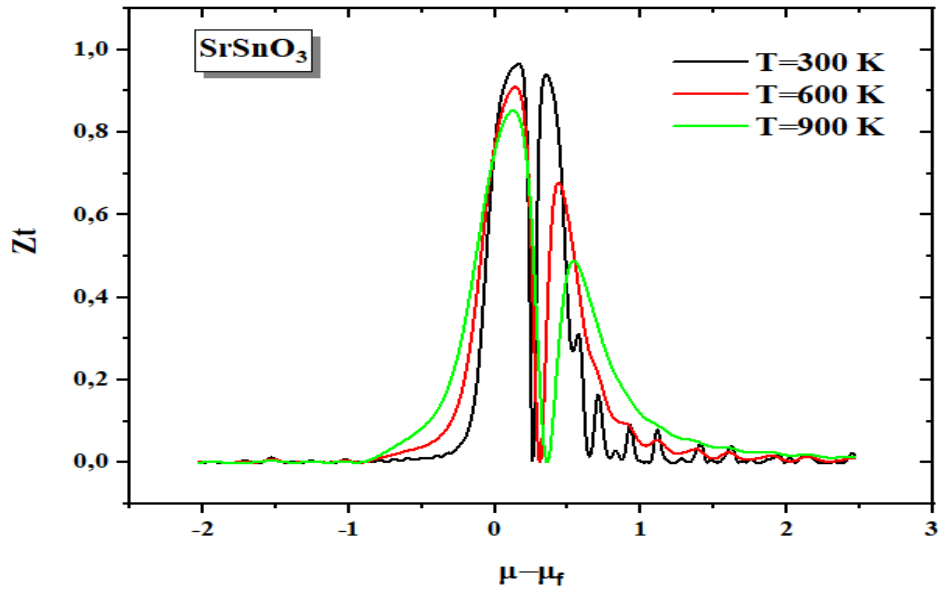

Figure (II.11): Electrical conductivity of the compound $SrSnO_3$ at different temperatures as a function of changes in chemical doping.

[1] A. Görling, Density-functional theory beyond the Hohenberg-Kohn theorem, Phys. Rev. A. 59 (1999) 3359–3374. https://doi.org/10.1103/physreva.59.3359.

[2] P. Hohenberg, W. Kohn, Inhomogeneous Electron Gas, Phys. Rev. 136 (1964) B864–B871. https://doi.org/10.1103/physrev.136.b864.

[3] Á. Nagy, Density functional. Theory and application to atoms and molecules, Phys. Rep. 298 (1998) 1–79. https://doi.org/10.1016/s0370-1573(97)00083-5.

[4] B.T. Sutcliffe, The Fundamentals of Electron Density, Density Matrix and Density Functional Theory for Atoms, Molecules and the Solid State — A Forum Preview, Fundam. Electron Density Density Matrix Density Funct. Theory At. Mol. Solid State. (2003) 3–8. https://doi.org/10.1007/978-94-017-0409-0_1.

[5] R.G. Parr, Density Functional Theory of Atoms and Molecules, Horiz. Quantum Chem. (1980) 5–15. https://doi.org/10.1007/978-94-009-9027-2_2.

[6] T.A. Wesołowski, Hohenberg-Kohn-Sham Density Functional Theory, Chall. Adv. Comput. Chem. Phys. (n.d.) 153–201. https://doi.org/10.1007/1-4020-5372-x_2.

[7] J.C. Slater, Damped electron waves in crystals, Phys. Rev. 51 (1937) 840.

[8] D.D. Koelling, G.O. Arbman, Use of energy derivative of the radial solution in an augmented plane wave method: application to copper, J. Phys. F Met. Phys. 5 (1975) 2041.

[9] O.K. Andersen, Linear methods in band theory, Phys. Rev. B. 12 (1975) 3060.

[10] D.R. Hamann, Semiconductor charge densities with hard-core and soft-core pseudopotentials, Phys. Rev. Lett. 42 (1979) 662.

[11] D. Singh, H. Krakauer, H-point phonon in molybdenum: Superlinearized augmented-plane-wave calculations, Phys. Rev. B. 43 (1991) 1441.

[12] E. Sjöstedt, L. Nordström, D.J. Singh, An alternative way of linearizing the augmented plane-wave method, Solid State Commun. 114 (2000) 15–20.

[13] P. Blaha, K. Schwarz, G. Madsen, D. Kvasnicka, J. Luitz, Wien2k, (2001).

[14] J.P. Perdew, K. Burke, M. Ernzerhof, Generalized Gradient Approximation Made Simple, Phys. Rev. Lett. 77 (1996) 3865–3868. https://doi.org/10.1103/physrevlett.77.3865.

[15] O.K. Andersen, T. Saha-Dasgupta, Muffin-tin orbitals of arbitrary order, Phys. Rev. B. 62 (2000) R16219.

[16] G.K. Madsen, D.J. Singh, BoltzTraP. A code for calculating band-structure dependent quantities, Comput. Phys. Commun. 175 (2006) 67–71.

[17] V.L. A. Otero-de-la-Roza, D. Abbasi-Pérez, Gibbs2: A new version of the quasiharmonic model code. II. Models for solid-state thermodynamics, features and implementation, Comput. Phys. Commun. 182(10) (2011) 2232–2248.

[18] V.L. A. Otero-de-la-Roza, Gibbs2: A new version of the quasi-harmonic model code. I. Robust treatment of the static data, Comput. Phys. Commun. 182(8) (2011) 1708–1720.

[19] F. Izumi, K. Momma, Three-dimensional visualization in powder diffraction, in: Solid State Phenom., Trans Tech Publ, 2007: pp. 15–20.

[20] K. Momma, F. Izumi, VESTA 3 for three-dimensional visualization of crystal, volumetric and morphology data, J. Appl. Crystallogr. 44 (2011) 1272–1276.

[21] K. Momma, F. Izumi, VESTA: a three-dimensional visualization system for electronic and structural analysis, J. Appl. Crystallogr. 41 (2008) 653–658.

[28] S. Saad Essaoud, Les composés à base de manganèse: investigation théorique des propriétés structurales électroniques et magnétiques, 2020. https://doi.org/10.13140/RG.2.2.30742.68169.

[29] S.S. Essaoud, A.S. Jbara, First-principles calculation of magnetic, structural, dynamic, electronic, elastic, thermodynamic and thermoelectric properties of Co2ZrZ (Z= Al, Si) Heusler alloys, J. Magn. Magn. Mater. (2021) 167984.

[30] O. Volnianska, P. Boguslawski, Magnetism of solids resulting from spin polarization of p orbitals, J. Phys. Condens. Matter. 22 (2010) 073202. https://doi.org/10.1088/0953-8984/22/7/073202.

[31] J.M.D. Coey, ed., Magnetism of localized electrons on the atom, in: Magn. Magn. Mater., Cambridge University Press, Cambridge, 2010: pp. 97–127. https://doi.org/10.1017/CBO9780511845000.005.

[32] M.D. Johannes, I.I. Mazin, Microscopic origin of magnetism and magnetic interactions in ferropnictides, Phys. Rev. B. 79 (2009) 220510.

[33] M. Valant, T. Kolodiazhnyi, I. Arčon, F. Aguesse, A.-K. Axelsson, N.M. Alford, The Origin of Magnetism in Mn-Doped SrTiO3, Adv. Funct. Mater. 22 (2012) 2114–2122.

[34] J. Degauque, Magnétisme et matériaux magnétiques: introduction, J. Phys. IV. 2 (1992) C3-1.

[35] P. Langevin, Sur la théorie du magnétisme, J PhysTheorAppl. 4 (1905) 678–693.

[36] A.T. Petit, P.L. Dulong, Recherches de la theorie de la chaleur, Ann Chim Phys. 10 (1819) 395–413.

[37] I.M. Abdel-Motaleb, S.M. Qadri, Thermoelectric Devices: Principles and Future Trends, ArXiv170407742 Cond-Mat. (2017). http://arxiv.org/abs/1704.07742 (accessed January 18, 2021).

[38] ديلمي, تحليل المبدأ الأول للخصائص الفيزيائية للمواد الفائقة التوصيل, PhD Thesis, Université de M’sila, 2020.

CONCLUSION

Conclusion

During the conducted research, we studied the physical properties of the SrSnO3 compound, focusing on the impact of temperature on its electrothermal properties. This was done using the semiclassical Boltzmann model and the Debye quasi-harmonic model to extract the effects of temperature and pressure on some thermal properties.

We initially verified its structural properties to determine its compressibility coefficient and structural properties at the most stable state. Additionally, we examined its electronic behavior based on the Density Functional Theory (DFT).

The results obtained indicated that the compound possesses highly distinctive properties, starting from its stable structural properties to its good compressibility coefficient, semi-metallic electronic behavior, and small band gap.

SrSnO3 is distinguished by its good thermal properties, as it exhibits average heat absorption (heat capacity) and minimal thermal expansion coefficient.

The compound also displayed favorable electrothermal properties such as the Seebeck coefficient, electrical conductivity, and thermal conductivity, making it a promising candidate for numerous electrothermal applications.

ملخص

في عملنا هذا أجرينا دراسة نظرية لحساب الخواص البنيوية ، الإلكترونية ، الترموديناميكية والكهروحرارية للمركب $SrSnO_3$ بإستعمال طريقة الأمواج المستوية المتزايدة خطيا(FP-LAPW) المعتمدة على نظرية دالية الكثافة(DFT).لحساب الكمون تبادل-ارتباط استعملنا تقريب التدرج المعمم *GGA* في دراسة خواص المركبين .في حساب الخواص البنيوية، قمنا بحساب ثابت الشبكة، معامل الانضغاطية ولفهم السلوك الإلكتروني لكلا المركبين قمنا بتحليل بنية عصابات الطاقة الإلكترونية وأطياف الكثافة الحالات الإلكترونية DOS) الكلية والجزئية. في حساب الخواص الترموديناميكية، ركزنا على حساب بعض المقادير الحرارية معينة باستخدام نموذج ديباي الشبه التوافقي ، حيث سمح لنا بدراسة تأثير درجة الحرارة والضغط على بعض المقادير مثل السعات الحرارية C_v ، معامل التمدد الحراري α ،الأنتروبيا.في نهاية قمنا بحساب الخواص الكهروحرارية كمعامل سيباك والناقلية الكهربائية الإلكترونية والناقلية الحرارية الالكترونية.

Abstract

In our work, we conducted a theoretical study to calculate the structural, electronic, thermodynamic, and thermoelectric properties of the SrSnO3 compound using the full-potential linearized augmented plane wave (FP-LAPW) method based on density functional theory (DFT). To calculate the exchange-correlation potential, we used the generalized gradient approximation (GGA) to study the properties of the compounds. In calculating the structural properties, we determined the lattice constant and the bulk modulus. To understand the electronic behavior of both compounds, we analyzed the electronic band structure and the density of states (DOS), both total and partial. In calculating the thermodynamic properties, we focused on determining certain thermal quantities using the quasi-harmonic Debye model, which allowed us to study the effect of temperature and pressure on quantities such as heat capacities Cv, thermal expansion coefficient α, and entropy. Finally, we calculated the thermoelectric properties such as the Seebeck coefficient, electronic electrical conductivity, and electronic thermal conductivity.